Silencing of ATF3 in primary cortical cultures derived from neonatal opossum Monodelphis domestica

Ivaničić, Matea

UNIVERSITY OF RIJEKA

DEPARTMENT OF BIOTECHNOLOGY

Master's program

Biotechnology in Medicine

Matea Ivaničić

Silencing of ATF3 in primary cortical cultures derived from neonatal opossums *Monodelphis domestica*

Master's thesis

Rijeka, 2021

UNIVERSITY OF RIJEKA

DEPARTMENT OF BIOTECHNOLOGY

Master's program

Biotechnology in Medicine

Matea Ivaničić

Silencing of ATF3 in primary cortical cultures derived from neonatal opossums *Monodelphis domestica*

Master's thesis

Mentor: Prof. Miranda Mladinić Pejatović, PhD

Co-mentor: Assist. Prof. Jelena Ban, PhD

Rijeka, 2021

SVEUČILIŠTE U RIJECI

ODJEL ZA BIOTEHNOLOGIJU

Diplomski sveučilišni studij

Biotehnologija u medicini

Matea Ivaničić

Utišavanje ATF3 u primarnim kulturama korteksa neonatalnog oposuma *Monodelphis domestica*

Diplomski rad

Mentor rada: prof. dr. sc. Miranda Mladinić Pejatović

Komentor rada: doc. dr. sc. Jelena Ban

Rijeka, 2021.

Acknowledgments

I wish to thank my mentor, Prof. Miranda Mladinić Pejatović, for accepting me as a part of the team in her Laboratory for Molecular Neurobiology. My work there in the last three years have nurtured my love and passion for science, and I will be forever grateful for the opportunity she gave me!

I would also like to thank my co-mentor, Assist. Prof. Jelena Ban, for sharing her knowledge, and for generous advice and support at any time.

I am especially grateful to my colleagues and friends, PhD students Antonela and Ivana. For their guidance and limitless patience, and for sharing their knowledge and priceless experience with me. It was a pleasure working with you, but also becoming your friend!

My biggest support during all these time at the university was my colleague, friend, and a laboratory partner Marta. Her positivity, thriving for knowledge, endless motivation, excellence, and love for science made these years easier, happier, and brighter. I like to believe that the slight competition between us made us both into our best selves!

A big thank you also to Katarina. Without Marta and her I wouldn't know what a real student life is. We spent together every minute in- and outside the classroom. We studied together. We travelled together.

Thank you for all the best memories!

Biggest love and thank you to Leon ♡

Master’s thesis was defended on September 29th, 2021

in front of the committee:

1. Assist. Prof. Nicholas J. Bradshaw, PhD, Committee Head
2. Assoc. Prof. Antonija Jurak Begonja, PhD, Committee Member
3. Prof. Miranda Mladinić Pejatović, PhD, Committee Member (Mentor)
4. Assist. Prof. Jelena Ban, PhD, Committee Member (Co-mentor)

This thesis has 67 pages, 25 figures, 8 tables and 49 references.

ABSTRACT

The mammalian central nervous system (CNS) develops primarily during the embryonal period, but final structuring and tuning occurs postnatally. Before or soon after birth, the mammalian CNS loses its ability to fully regenerate after injury. Therefore, neuroregeneration studies are mostly conducted on rodent embryos (mice or rats) or derived *in vitro* preparations, such as primary cell or tissue cultures. However, an intrauterine surgical procedure is necessary to access rodent embryos, which usually means sacrificing the mother - an ethically questionable issue. Therefore, to study regenerative mechanisms of the CNS, we have used an alternative experimental animal: the grey South American short-tailed opossum (*Monodelphis domestica*), a marsupial without a pouch. Opossum neonates are very immature, and their CNS develops mostly postnatally, with the cortical plate not observed until postnatal day (P)3-5. Therefore, harming the mother is not necessary in order to investigate CNS development in opossums. Furthermore, opossums are unique among mammals in their ability to successfully regenerate the spinal cord after injury during the first two weeks of their life. After that period, the regenerative capability of their spinal tissue is lost. Thus, the first aim of this work was to characterize primary cortical cell cultures obtained from opossums at two developmentally different ages, P3-5 and P16-18, using immunofluorescent microscopy. The results showed a high percentage of neurons in primary cultures derived from both P3-5 and P16-18 opossums (>96% and >80% at DIV7, respectively). The second aim was to genetically silence activating transcription factor 3 (ATF3) in opossum primary cortical cultures, via transfection with specific siRNA molecules, to further investigate its role in neuroregeneration. The cell transfection protocol was optimized to reach the optimal transfection efficiency, and the ATF3 gene and protein levels were assessed with quantitative real-time PCR and Western blot, respectively. Altogether, the results indicate that primary cortical cultures obtained from opossum *M. domestica* are favorable preparation that can be used to investigate mechanisms underlying CNS regeneration, particularly the involvement of regeneration-related transcription factors, such as ATF3.

Key words: opossum, primary cell culture, CNS regeneration, ATF3, gene silencing

SAŽETAK

Središnji živčani sustav (SŽS) sisavaca se razvija primarno tijekom embrionalnog razvoja, a funkcionalno sazrijevanje živčanih mreža i procesa događa se postnatalno. Prije ili nedugo nakon rođenja, sisavci gube sposobnost potpune regeneracije SŽS-a nakon ozljede. Većina istraživanja regeneracije SŽS-a provodi se na embrijima glodavaca (miševa ili štakora) ili *in vitro* preparatima, poput primarnih staničnih ili tkivnih kultura. Embrijima se ne može pristupiti bez intrauterine operacije, a to obično podrazumijeva žrtvovanje majke što je etički upitno. Iz tog razloga, za istraživanje regenerativnih mehanizama SŽS-a odlučili smo se za alternativni organizam: sivi kratkorepi oposum (*Monodelphis domestica*), tobolčar bez posteljice. Mladunci oposuma se rađaju vrlo nezreli, te se njihov SŽS većinom razvija postnatalno, kortikalnu ploču, primjerice, nije moguće uočiti do postnatalnog dana (P)3-5. Dakle, razvoj SŽS-a se kod oposuma može istraživati bez potrebe da se pritom šteti majci. Nadalje, oposumi su posebni među sisavcima jer u prva dva tjedna života mogu uspješno regenerirati leđnu moždinu nakon ozljede. Nakon tog razdoblja, mogućnost regeneracije moždanog tkiva se gubi. Stoga, prvi cilj ovog rada je bio pomoću imunofluorescentne mikroskopije opisati primarne stanične kulture korteksa pripremljene od dvije razvojno različite dobi oposuma, starih P3-5 i P16-18. Rezultati su pokazali visok postotak neurona u staničnim kulturama pripremljenih od P3-5 (>96%) i P16-18 (>80%) oposuma nakon 7 dana u kulturi. Drugi cilj bio je genetski utišati aktivirajući transkripcijski faktor 3 (ATF3) u primarnim staničnim kulturama korteksa oposuma koristeći metodu transfekcije sa specifičnim siRNA molekulama, kako bi se pobliže istražila njegova uloga u neuroregeneraciji. Protokol je bio optimiziran kako bi se postigla optimalna učinkovitost transfekcije, a razine ATF3 mRNA i proteina, bile su provjerene kvantitativnim PCR-om u realnom vremenu, odnosno Western blot-om. Zaključno, rezultati ovog rada ukazuju na to da su primarne stanične kulture korteksa oposuma *M. domestica* poželjan preparat za istraživanje mehanizama regeneracije SŽS-a, osobito u istraživanju uloge transkripcijskih faktora povezanih s regeneracijom kao što je ATF3.

Ključne riječi: oposum, primarna stanična kultura, regeneracija SŽS-a, ATF3, utišavanje gena

CONTENTS

1. INTRODUCTION

1.1. Central nervous system pathologies

Alzheimer's disease (AD), Parkinson's disease (PD), schizophrenia, depression, epilepsy, cerebral palsy, spinal paralysis, and stroke are some of the most common disorders that affect the central nervous system (CNS). In the United States of America, more people are hospitalized because of neurological or mental disorders than because of any other group of diseases (1). CNS pathologies are an enormous financial burden on patients and health systems. Furthermore, the therapies available are limited and a lot of them are still in the experimental phase, which are not available and/or affordable for everyone. However, when there is a little or no hope for recovery from the disease, the emotional burden on patients and their families is far greater than just the economic aspects described.

CNS disorders cannot be prevented and effectively treated without at least a basic understanding of CNS physiology. Thus, knowledge collected from neuroscience research is important and is growing exponentially. Increasingly effective treatments for PD (2), depression (3) and schizophrenia (4) are being developed, while strategies for rescuing dying neurons and potentiating regenerative processes in AD patients (5) and patients who suffered from a stroke (6) are being tested.

1.1.1. CNS diseases

CNS diseases affect the brain and/or the spinal cord. Brain diseases can roughly be divided into developmental, neuropsychiatric and neurodegenerative diseases, as well as brain tumors and infections (1). The latter are relatively rare due to immune privilege (7) of the brain, as well as currently available therapies and advances of modern medicine. The brain is considered "immune privileged" because it is protected by the blood-brain barrier (BBB) and the immune system in the brain is

suppressed compared to the rest of the body. The BBB consists of tight junctions between brain vasculature endothelial cells, the basal lamina of endothelial cells and the ends of astrocyte processes (7). The BBB consistently protects the brain from pathogens, immune cells and various factors that could enter through the blood.

Among these types of CNS diseases, neurodegenerative diseases are estimated to be the most common. The following three paragraphs provide a brief overview of the epidemiology and characteristics of Alzheimer's, Parkinson's and Huntington's disease (HD).

AD makes up 60-80% of all cases of dementia and it is estimated to affect 24 million people globally (8). Two typical neuropathological features, the accumulation of extracellular plaques, made of 42-amino-acid amyloid-beta, and intracellular neurofibrillary tangles of hyperphosphorylated microtubule-associated tau protein, are found in AD patients' brains. Since anatomical distribution of these pathologies can vary, AD clinical phenotypes are extremely heterogeneous (5).

PD is the second most common neurodegenerative disease, with an estimate that it affects 3% of the population older than 80 and 0.3% of the overall population. PD patients develop a wide range of motor symptoms, such as bradykinesia, resting tremor, rigidity, and postural instability. Neuropathological changes in the affected brain usually include the loss of dopaminergic neurons in the substantia nigra and the formation of so-called Lewy bodies. Lewy bodies are eosinophilic, intracytoplasmic neuronal inclusions that contain insoluble aggregates of α-synuclein and ubiquitin (8).

HD is an autosomal dominant neurodegenerative disorder that is caused by excessive expansion of CAG repeats in the huntingtin gene on chromosome 4. Its symptoms manifest as involuntary movements, personality changes and dementia and they start to develop in relatively

younger people. On average, it is diagnosed in people 40 years old, and the yearly incidence is estimated to be 0.38 cases per 100,000 people (8).

1.1.2. CNS injury

The two most common types of CNS injuries are traumatic brain injury (TBI) and spinal cord injury (SCI). TBI is the disruption of brain activity due to an external force or violent impact to the head (9) and SCI results from a sudden impact to the spine that fractures or dislocates vertebrae (10). Based on the number of people that sought medical care after injury, it is estimated that there are around 55 million people suffering from TBI and around 27 million people with SCI in the world. TBI and SCI give a poor prognosis for recovery, and the medical care they require is complex and expensive. The most common causes of CNS injuries are falls, road injuries and interpersonal violence, such as gunshot wounds or war (11).

TBI leads to long-term cognitive and behavioral deficits, and to an increased risk for developing neurodegenerative disorder(s). It can also have consequences on other organ systems such as hormonal dysfunction and disrupted bone metabolism (9,12).

SCI can happen in any part of the spinal cord, from cervical to sacral. Depending on the severity of the injury, it can cause loss of function below the lesion site. Loss of function is usually permanent, making the patient severely disabled and susceptible to numerous secondary illnesses (13).

In the 19th century, brain injury was known to disrupt movement, sensations and thought, and that it can cause death. Today we know that that main reasons for a fatal outcome are the inability of CNS axons to regenerate after injury and insufficient generation of new neurons (1).

When CNS injury occurs, the processes that follow can be divided into events called primary injury and secondary injury. Primary injury (12) is caused by the initial mechanical forces delivered to the CNS tissue, and its

extent determines the outcome and severity of the injury. Additionally, blood vessels, axons, and glial processes at the site of injury are sheared. In both SCI and TBI, mechanical deformation of the tissue results in instant and thus, necrotic, cell death. Secondary CNS injury (10,12) begins immediately after the primary injury, and it lasts for weeks or months, causing progressive damage. Generally, secondary injury refers to a series of cellular, molecular, and biochemical processes that continue to self-destruct the CNS tissue after injury, while reducing the chances of recovery. Secondary injury is divided into acute, sub-acute and chronic phases. The acute phase starts immediately after the primary injury and is characterized by a series of events such as vascular damage, disrupted ionic balance, excitotoxicity, calcium influx, generation of free radicals and oxidative stress, lipid peroxidation, inflammation, edema, and necrotic cell death. As the injury progresses, the sub-acute phase of secondary injury begins. This phase is characterized by a series of destructive processes such as cell death by apoptosis, demyelination of surviving axons, retrograde degeneration of the distal end of an axon, retraction bulb formation, extracellular matrix remodeling, and evolution of a glial scar at the site of an injury. Eventually, the chronic phase occurs, which involves the formation of a cystic cavity, progressive axonal dieback, and maturation of the glial scar. Also, there is an increased risk of infection at the injured site since post-injury events disrupt the consistency of the BBB.

1.2. CNS regeneration

In early neuroanatomical research, the adult mammalian CNS was considered incapable of regeneration (1). Neurons are post-mitotic cells, which means that they do not divide, and their number is limited.

During development, neurons are generated from neural progenitor cells (NPCs). NPCs include neuroepithelial cells and basal progenitors. Neuroepithelial cells are present at the earliest embryonic stages and from

them both basal progenitors and RGCs are generated. Basal progenitors are neurogenic in the early embryonic stage, while in later embryonic stages they mostly generate non-neuronal CNS cells – astrocytes and oligodendrocytes. RGCs are distributed in various brain regions and they generate most of the neurons in the midneurogenesis phase (14). In the developing cerebral cortex, RGCs function both as NPCs and as guides for neuronal migration, as Götz et al. (15) have reported, and these processes are regulated by the expression of the paired box-6 (Pax6) gene.

Eventually, more and more evidence indicated the presence of two brain regions in which regeneration occurs even in adulthood: the subventricular zone (SVZ) and the subgranular zone (SGZ). Formation of new neurons was also found in various brain regions such as the basal forebrain, striatum, subcortical white matter, and hypothalamus. In these brain regions, after injury, interaction of non-neuronal cells, certain proteins and factors induces progenitor cell differentiation, as well as migration and integration of newly produced cells into the lesioned site (16). Although these findings seem promising, the intrinsic regenerative capacities of the adult mammalian CNS are not sufficient in the case of traumatic injury or to overcome chronic pathological changes that occur in neurodegenerative diseases.

CNS neuroregeneration implies generation of new neurons, a process that physiologically occurs during CNS development, and re-growth of injured axons. Thus, investigation of CNS developmental mechanisms may help to understand underlying processes of neuroregeneration, and potentially allow us to manipulate them in order to treat CNS pathologies such as neurodegenerative diseases and CNS injuries. Another approach is to investigate axonal regeneration in the peripheral nervous system (PNS), which occurs naturally, and to determine the molecular, cellular and extracellular differences between regenerating PNS and non-regenerating CNS.

1.3. *Monodelphis domestica* in neuroregeneration studies

The grey short-tailed opossum (*Monodelphis domestica*) is a pouchless marsupial. Its natural habitat is the South American countries Brazil, Bolivia, Paraguay, and Argentina. Opossums breed during the whole year and have up to 6 litters per year, with up to 11 neonates per litter. Neonates are born approximately 14 days after conception, and they stay attached to the nipple for another 14 days. Young opossums are weaned at approximately postnatal day (P)56 (17).

CNS development in opossums starts before birth and finishes postnatally. Saunders et al. (18) and Puzzolo & Mallamaci (19) investigated postnatal neuro- and gliogenesis in *M. domestica*. Saunders et al. (18) tracked the development of the neocortex in the *M. domestica* brain from birth to adulthood and found that the cortical plate was not present until P3-5. Therefore, complete cortical development can be studied in postnatal opossums. A transcriptomic study by Cardoso-Moreira et al. (20) reported that opossums at P3-5 correspond to embryonal day (E)15.5-18.5 rats or E14-16 mice, and that P16-18 opossums correspond to P1-2 rats or mice, indicating the immaturity of opossum neonates. Moreover, opossums can successfully regenerate their spinal cord after injury in the first two weeks of their life, after which the regenerative ability of their spinal tissue is lost (21,22). Differences in gene expression, epigenetics and/or posttranslational modifications of proteins between developmentally different ages (Figure 1) could point out the key mechanisms involved in regeneration of CNS, making opossum a favorable organism to study regenerative mechanisms.

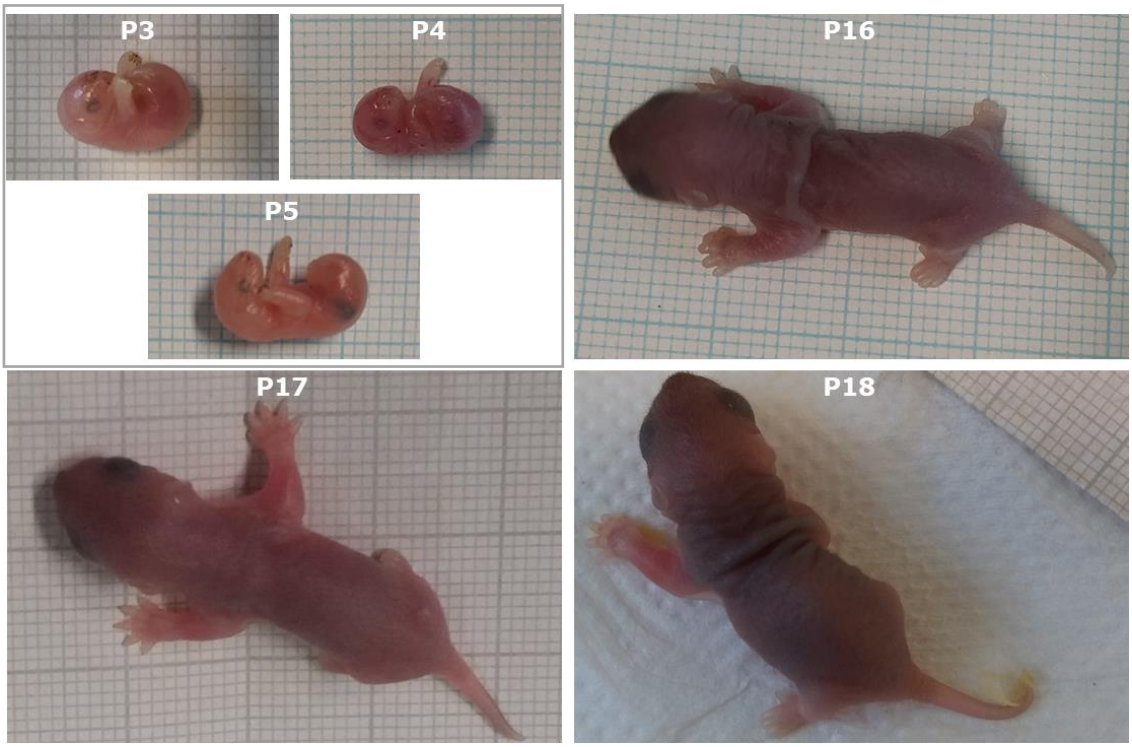

Figure 1 ***Opossum neonates are very immature.*** *Opossum (*Monodelphis domestica*) pups that (P3-5) can and (P16-18) cannot regenerate their spinal cord after injury.*

1.4. ATF3

Activating transcription factor 3 (ATF3) is a member of the ATF/cAMP responsive element binding (ATF/CREB) protein family of transcription factors. Proteins of the ATF/CREB family regulate eukaryotic gene expression by binding to a short DNA sequence (TGACGTCA) in promoter regions. This sequence is called the ATF/CREB consensus sequence. All members of the ATF/CREB family bind DNA with a similar, basic leucine zipper (bZip) domain, and they can form homodimers, or heterodimers with other members of the family (23). ATF3 is induced under stress conditions in different cell types and affects their survival, proliferation, and death.

According to the information available in the Ensembl (24) database, human ATF3 gene is located on the q arm of the chromosome 1 and has 11 transcript variants, 8 of which are protein coding. Since in this work opossums were used, human ATF3 was compared to opossum ATF3. ATF3

splice variants and respective protein sequences (Table 1) were compared using data available in Universal Protein Resource (Uniprot) database[1].

Table 1 ***Human and opossum ATF3 gene transcripts and their products.***

organism	splice variant (Ensembl entry)	protein isoform (Uniprot entry)	size (aa)	size (kDa)
H. sapiens	**ATF3-202, -206**	**P18847-1**	**181**	**22**
H. sapiens	ATF3-210, -211	P18847-5	124	14
M. domestica	**ATF3-201**	**A0A5F8HAS1**	**181**	**22**
M. domestica	ATF3-202	F6Q0B9	124	14

According to human ATF3 Uniprot entries, the full-length protein isoform can have 3 different posttranslational modifications (PTMs): SUMOylation of lysine 78 (Lys78) and lysine 175 (Lys175), and phosphorylation of threonine 162 (Thr162). SUMOylation and phosphorylation are reversible PTMs. SUMOylation is the covalent binding of a small ubiquitin-like modifier (SUMO), and it adds approximately 12 kDa to the mass of a protein. Phosphorylation is the addition of a phosphate group, usually to a serine (Ser), threonine (Thr) or Tyrosine (Tyr) hydroxyl group, and it adds around 1 kDa to the mass of a protein. An alternatively spliced 14 kDa isoform lacks 64 amino acids from the C-terminus and it can only have the Lys78 PTM.

1.4.1. Role in neuroregeneration

ATF3 is almost undetectable in neurons under physiological conditions. However, after PNS axonal injury, its expression increases, and it acts in a neuroprotective manner. It induces survival and expression of

[1] https://www.uniprot.org/

growth-associated genes, prevents cell death and promotes neurite formation and elongation (25). In CNS, ATF3 is upregulated in injured neurons, and Campbell et al. (26) showed that upregulation also occurs in CNS neurons when they are regenerating their axons into peripheral nerve grafts in the thalamus.

The role of ATF3 in neuroprotection and peripheral nerve regeneration has been extensively described. Overexpression of ATF3 is neuroprotective in mouse models of amyotrophic lateral sclerosis (ALS) (25) and neuronal models of excitotoxicity (27). Furthermore, upregulation of ATF3 alone was sufficient to protect primary cortical neurons from proline-arginine (PR) toxicity (28). ATF/CREB transcription factors, including ATF3, and regeneration associated genes, such as c-*jun*, STAT3 and SMAD1, orchestrate axonal regeneration after PNS injury. ATF3 promotes axonal maintenance, dynamic axonal sprouting, and remodeling (25).

In contrast, axons in the adult CNS show relatively limited response to injury, despite ATF3 upregulation. Initial sprouting occurs, but is soon terminated (26) and ends with the formation of retraction bulb (29). CNS environment and intrinsic factors both diminish regenerative abilities of the CNS neurons. Inhibitory molecules secreted by oligodendrocytes and astrocytes form the glial scar, disturb axonal re-growth, and negatively contribute to CNS neuronal recovery. In addition, central axons gradually lose their intrinsic growth ability during maturation (29).

1.5. Transfection

1.5.1. Different methods of transfection

Transfection is a method used to deliver foreign nucleic acids into eukaryotic cells using nonviral vectors. The nucleic acid can be either DNA, such as DNA fragment integrated in a plasmid vector, or RNA molecule, such a mRNA or siRNA. The target gene can be wild-type or a mutant

version of the gene, and the experiment can be designed to achieve different outcomes.

Depending on how long it lasts, transfection can be either stable or transient. Stable transfection is successfully performed when the transfected material, usually part of a plasmid DNA, enters the nucleus and integrates into the cellular genome, or when a plasmid DNA stays in the cytoplasm as an episomal entity. In both scenarios, cells gain a new characteristic. If cells proliferate, this characteristic will pass on to the new cell generation. In transient transfection, the nucleic acid delivered is present in the cell for a limited time, usually for a few days, and is not integrated into the genome. Therefore, in the case of proliferating cells, transiently transfected genetic material does not pass on to the new generation of cells.

Transfection methods are divided into physical and chemical methods, depending on how the nucleic acid is inserted into the cell (30). Physical methods, such as electroporation or sonoporation, physically disturb the cell membrane, enabling foreign nucleic acid to enter the cell. Chemical methods use a specific chemical, either lipid or non-lipid, to aid in transfection. Lipid-based transfection reagents contain a cationic lipid that fuses with negatively charged nucleic acid. Non-lipid-based transfection reagents are divided into several classes such as micro-/nano-particles, peptides, polymeric-based transfection reagent, calcium phosphate, and dendrimers. In this work, a lipid-based transfection reagent was used.

1.5.2. Liposomal carrier membrane fusion

Lipid-based transfection reagents deliver their cargo through two main processes: endocytosis and direct fusion with the cell membrane. The transfection method used in this work is a lipid-based method called liposomal carrier membrane fusion (Figure 2).

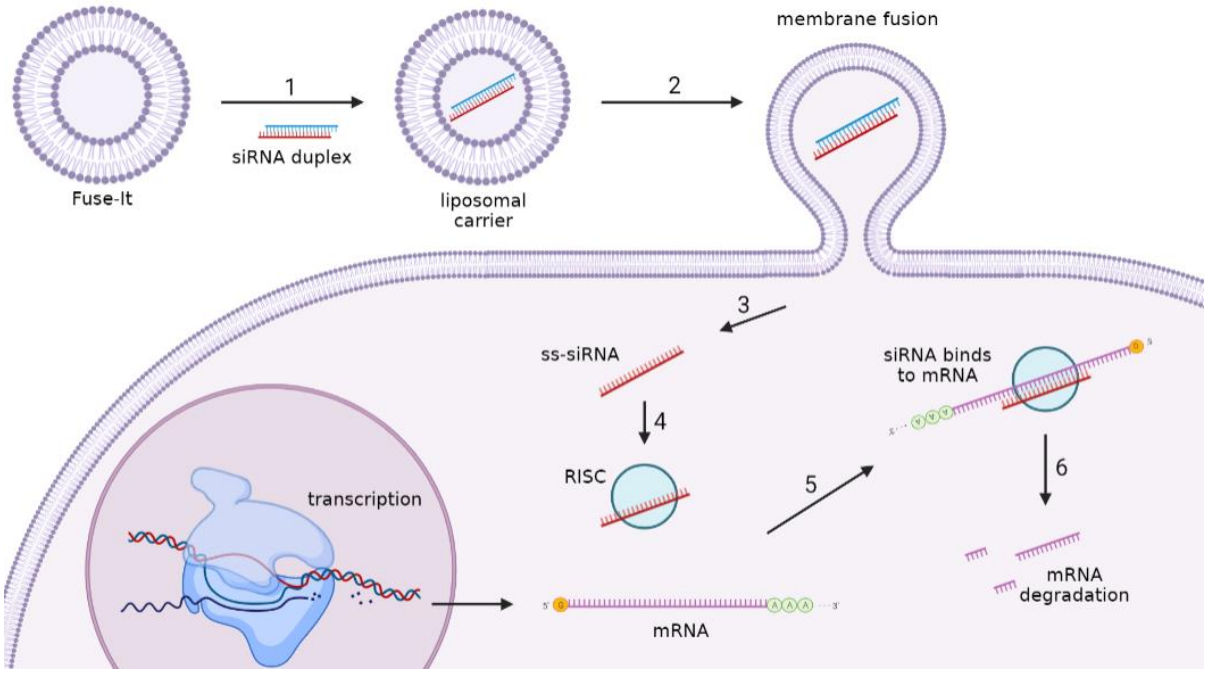

Figure 2 ***Schematic representation of siRNA cell transfection.*** *1) siRNA duplex is neutralized and fused with liposomal carrier. 2) Liposomal carrier fuses with the cell membrane. 3) siRNA duplex enters the cytoplasm directly, where it is processed into single strand (ss)-siRNA by dicer. 4) RNA-induced silencing complex (RISC) binds ss-siRNA. 5) siRNA binds complementary to mRNA and 6) mRNA degrades. Illustration created with BioRender.com.*

Fuse-It liposomal carrier (see Materials and Methods) is cargo-specific, in our case siRNA-specific. It attaches and fuses with cell membrane easily, due to its similar physicochemical properties. The siRNA duplex immediately enters the cytoplasm and the dicer enzyme processes it into single stranded (ss)-siRNAs. RNA-induced silencing complex recognizes and binds ss-siRNA, and siRNA then binds to the complementary sequence on mRNA molecule. mRNA is degraded if siRNA binds with a near perfect complementarity and, when mismatches are present, translational repression occurs.

Delivering siRNA through membrane fusion has a few advantages compared to endocytosis. The transfection is faster because siRNA enters the cell cytoplasm directly after liposomal carrier membrane fusion. When liposomal carriers enter the cells through endocytosis, an endosome forms.

The endosome then fuses with a lysosome, and siRNA is delivered into the cytoplasm after lysosomal degradation. siRNAs can easily be degraded in this process and, therefore, a higher concentration of siRNA is normally needed. Furthermore, carriers that fuse with cell membrane are biocompatible and cause low cytotoxicity.

2. AIMS AND HYPOTHESIS

AIMS

1. The first aim of the thesis was to prepare and characterize primary cortical neuronal cell cultures derived from neonatal opossums, *Monodelphis domestica*. Cultures were obtained from 3-5 and 16-18 days old animals. Our goal was to use these cultures as a novel *in vitro* platform to study regenerative mechanisms in mammals after CNS injury. The culturing protocol and characterization of opossum primary cortical cultures were recently published (31).
2. The second aim of the thesis was to choose one candidate molecule involved in neuroregeneration and to optimize the protocol for its gene silencing in newly developed opossum neuronal cortical cultures. Silencing of the candidate molecule will be used to investigate its role in neuronal regeneration. The molecule of interest was ATF3 (Mladinic et al., 2014 (33); Petrović et al., unpublished data), and it was silenced via transfection of the cell cultures with ATF3-specific siRNA molecules. This was the first ever attempt to transfect primary cortical cell cultures derived from *M. domestica* using siRNA. Therefore, most of the time and energy invested in this work was focused on the challenging establishment and optimization of this method.

HYPOTHESIS

The main hypothesis of this thesis is that neuroregeneration-related molecules, such as ATF3, can be successfully silenced in primary cortical cultures derived from *M. domestica* using specific siRNA molecules and that this procedure abolishes the molecule of interest at the RNA and the protein level.

3. MATERIALS AND METHODS

3.1. Animals

South American gray short-tailed opossum, *Monodelphis domestica*, pups of both sexes were used, at two developmentally different ages: P3-5 and P16-18. The opossum colony is maintained at the animal house facility of the University of Trieste. The guidelines of the Italian Animal Welfare Act were followed, and the use of opossums was approved by the Local Veterinary Service, the Ethics Committee board, and the National Ministry of Health (Permit Number: 1FF80.N.9Q3), following the European Union guidelines for animal care (d.1.116/92; 86/609/C.E.). The animals were housed in standard laboratory cages with controlled temperature (27-28°C) and humidity (50–60%), a 12/12-hour light/dark cycle and *ad libitum* access to food and water. All experiments described here were performed in accordance with the European Directive 2010/63/EU for animal experiments. All efforts have been made to minimize animal suffering and the number of animals used in experiments.

3.2. Primary cell cultures

All instruments and surfaces used were precleaned with 70% ethanol (Gram-mol, Zagreb, Croatia) and 1% Incidin (Ecolab, Zagreb, Croatia). All solutions were filter sterilized through a 0.22 µm syringe filter (Carl Roth, Karlsruhe, Germany).

3.2.1. Coverslips and plates preparation

For immunocytochemical analysis, 12 mm diameter coverslips (Thermo Fisher Scientific, Waltham, MA, USA) were treated with 1 M hydrochloric acid (HCl, Ru-Ve, Sv. Nedelja, Croatia) overnight at room temperature (RT, 20-22°C). Next day, coverslips were washed in distilled water to remove any traces of HCl, incubated in absolute ethanol for an hour at RT, and then dry sterilized at 150°C for 90 min. Sterile coverslips

were placed in a 24-well tissue culture plate (Sarstedt, Nümbrecht, Germany) and coated with 50 µg/mL poly-L-ornithine (PO, Sigma-Aldrich, St. Louis, MO, USA) overnight at 32°C. The following day, PO was removed, and coverslips were coated with 2 µg/mL laminin (Sigma-Aldrich) for 3-4 h at 32°C.

For cells intended for qPCR and Western blot analysis, wells of either a 24- or 6-well (Sarstedt) plate were coated with 50 µg/mL PO overnight at 32°C and removed immediately before plating of the cells.

3.2.2. Dissociation and plating of the cells

Primary cell cultures were prepared from cortices of postnatal opossums of two developmentally different age groups, P3-5 and P16-18. After decapitation with scissors, dissection was performed in ice-cold oxygenated (95% O_2/5% CO_2) Krebs solution (113 mM NaCl, 4.5 mM KCl, 1 mM $MgCl_2$ x $6H_2O$, 25 mM $NaHCO_3$, 1 mM NaH_2PO_4, 2 mM $CaCl_2$ x $2H_2O$, 11 mM glucose and 0.5% w/v Penicillin/Streptomycin/Amphotericin B, pH 7.4, all from Sigma–Aldrich). Both cortical hemispheres were used to obtain primary cells, while olfactory bulbs and remaining subcortical structures were removed. The meninges were removed from cortices with fine forceps. The dissected tissue was chopped into small pieces and washed three times with cold sterile phosphate-buffered saline (PBS) solution (137 mM NaCl, 2.7 mM KCl, 10 mM Na_2HPO_4, 2 mM KH_2PO_4, all from Sigma–Aldrich). Cortices were enzymatically digested with prewarmed (32°C) trypsin in EDTA (Santa Cruz Biotechnology, SCBT, Dallas, TX, USA). Cortices from P3-5 and P16-18 pups were digested in 0.5% w/v trypsin for 10 min and 2.5% w/v trypsin for 15 min, respectively, on a thermo block at 32.5°C. Samples were washed three times in PBS and cells were separated from the tissue in a trituration solution containing 10 mg/mL DNase I (Sigma–Aldrich), 1 mg/mL trypsin inhibitor (SCBT), and 1% w/v bovine serum albumin (BSA; Pan-Biotech, Aidenbach, Germany) in Hank's Balanced Salt Solution (HBSS) solution without Ca^{2+} and Mg^{2+} ions (Pan-Biotech). Trituration was performed by mechanical pipetting, with a 1 mL filter tip,

for at least 20 times to break the tissue structure. Larger pieces of the tissue were left to settle at the bottom of the tube and the supernatant was collected in a fresh tube. Trituration was repeated for additional two times. The supernatant containing dissociated cells was layered on top of 5% w/v BSA solution in HBSS. Cells were centrifuged at 100 x *g* for 5 min at RT and resuspended in 1 mL of plating medium, consisting of Dulbecco's Modified Eagle Medium (DMEM) with stable glutamine, supplemented with 10% w/v fetal bovine serum (FBS) and 1% w/v Penicillin/Streptomycin (all from Pan-Biotech). An additional 1 mL of the plating medium was added to the cell suspension, which was then transferred into the 35 mm Petri dish (Sarstedt) through a 70 µm cell strainer (Corning Inc., Corning, NY, USA) for preplating. Cells were incubated at 32°C for 5 min and collected. Before plating, cells were counted in the hemocytometer and the cell suspension was diluted in plating medium in 15 mL tubes (Carl Roth) to the density of 5×10^4 cells per well for 24-well plate or 5×10^5 cells per well for the 6-well plate.

In cultures for use in an immunofluorescence assay, 24 h after plating, 2/3 of the plating medium was replaced with fresh prewarmed neuronal medium containing Neurobasal medium, supplemented with B27 (both from Thermo Fisher Scientific), 1 mM L-glutamine and 1% Penicillin/Streptomycin (both from Pan-Biotech). Media was subsequently changed once per week, each time replacing half of the medium with fresh prewarmed neuronal medium.

Primary cortical cultures were maintained in an incubator at 32ºC with 5% CO_2 and 95% relative humidity. For easier visualization, a schematic overview of the procedure is given in Figure 3.

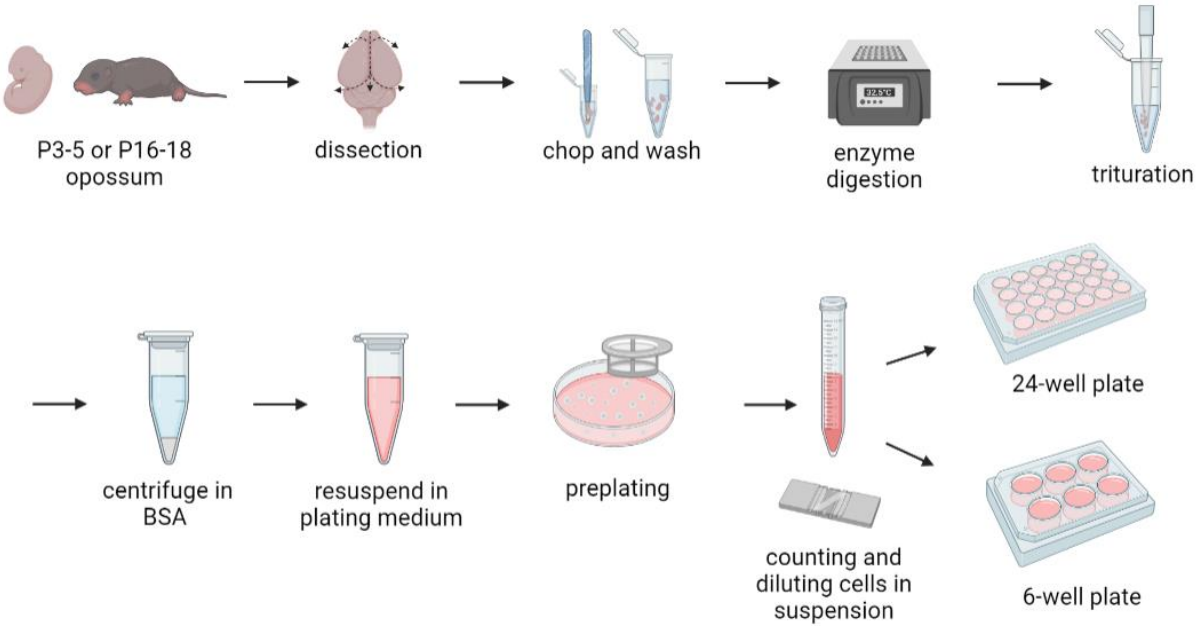

Figure 3 ***From animal to cell culture****. A schematic, simplified representation of the primary cortical cell culturing protocol. Illustration created with BioRender.com.*

3.3. Fluorescent immunocytochemistry assay

Coverslips with cells on them were washed in PBS and fixed with 4% paraformaldehyde (PFA) containing 200 mM sucrose (both Sigma-Aldrich) in PBS, pH 6.9, for 20 min at RT. Coverslips were washed 3x with PBS, saturated with 0.1 M glycine (VWR International, Radnor, PA, USA), permeabilized with 0.1% Triton X-100 (Sigma-Aldrich) and washed again in PBS. Each step lasted for 5 min. Cells were blocked with 0.5% w/v BSA in PBS for 30 min. Coverslips were then transferred into a "wet" chamber[2], incubated with primary antibodies (Table 2) for 1 h, and then washed two times in PBS. Coverslips were incubated with secondary antibodies conjugated with fluorophores (Table 3) and 300 nM 4',6-diamidino-2-phenylindole (DAPI, Thermo Fisher Scientific) for 30 min. DAPI was used for cell nuclei staining.

[2] An improvised, humid and dark chamber; used for incubations with antibodies.

Table 2 ***Primary antibodies used in this work.***

Primary antibody	Host and isotype	Dilution	Immunogen	Producer, Cat#, RRID	UniProt Identity
β-Tubulin III (TUJ1)	mouse monoclonal IgG_{2a}	1:200	microtubules derived from rat brain	Biolegend, 801201, AB_2313773	99.8%
microtubule-associated protein 2 (MAP2)	mouse monoclonal IgG_1	1:200	bovine MAP2	Sigma-Aldrich, M1406, AB_477171	82.8%
neuronal nuclei (NeuN)	rabbit monoclonal	1:200	synthetic peptide within Human NeuN aa1-100 (Cysteine residue)	Abcam, ab177487, AB_2532109	84.0%
synapsin I	rabbit polyclonal	1:100	synapsin I (a mixture of Ia and Ib) purified from bovine brain	Millipore, AB1543, AB_2200400	72.3%
glial fibrillary acidic protein (GFAP)	mouse monoclonal IgG_1	1:200	GFAP from porcine spinal cord	Sigma-Aldrich, G3893, AB_477010	84.9%
paired box 6 (Pax6)	rabbit polyclonal	1:100	synthetic peptide corresponding to Mouse Pax6, aa 267-285	Abcam, ab5790, AB_305110	100.0%

vimentin (vim)	mouse monoclonal IgG_1	1:300	full-length native protein	Abcam, ab8069, AB_306239	91.9%
vimentin (vim)	rabbit monoclonal IgG	1:400	synthetic peptide within Human Vimentin, aa 400 to the C-terminus	Abcam, ab92547, AB_10562134	91.9%

For F-actin staining, Phalloidin-iFluor 488 (Abcam, Cambridge, UK), diluted 1:500, was incubated for 30 min simultaneously with secondary antibodies. Primary and secondary antibodies, as well as Phalloidin-iFluor 488, were diluted according to the Tables 2 and 3, respectively, in 0.5% w/v BSA in PBS. Cells were finally washed two times in PBS and once in distilled water (dH_2O). All washing steps lasted for 5 min. All steps were performed at RT.

For the proliferation assay, the Click-iT 5-ethynyl-20-deoxyuridine (EdU) Cell Proliferation Kit with Alexa Fluor 488 dye was used (Thermo Fisher Scientific) according to the manufacturer's instructions. Briefly, EdU was added to the cells 24 h before the analysis. Cells were fixed (as described above) and, after the permeabilization step, immunolabeled for 30 min at RT in Click-iT reaction cocktail. The procedure then continued as in the classical fluorescent immunocytochemistry assay.

Coverslips were mounted face-down on glass slides prewashed with 70% ethanol. Mounting medium (Vectashield, Vector Laboratories, Burlingame, CA, USA) was applied on a glass slide in amounts of 3 µL per coverslip, and coverslips were sealed with nail polish.

For each primary antibody used, the similarity between the protein sequence of opossum and immunogen was compared in the UniProt database (see Table 2).

Table 3 ***Secondary antibodies used in this work.***

Secondary antibody	Fluorophore	Dilution	Producer, Cat#, RRID
goat anti-mouse	Alexa Fluor® 488	1:400	Thermo Fisher Scientific, A32723, AB_2633275
goat anti-mouse IgG_1	Alexa Fluor® 488	1:300	Thermo Fisher Scientific, A-21121, AB_2535764
goat anti-mouse	Alexa Fluor® 555	1:400	Thermo Fisher Scientific, A32732, AB_2633281
goat anti-rabbit	Alexa Fluor® 555	1:400	Thermo Fisher Scientific, A32732, AB_2633281
goat anti-mouse IgG_{2a}	Alexa Fluor® 555	1:300	Thermo Fisher Scientific, A-21137, AB_2535776
goat anti-rabbit	Alexa Fluor® 647	1:300	Abcam, ab150083, AB_2714032

3.3.1. Imaging

Imaging of the samples was performed with an Olympus IX83 inverted fluorescent microscope (Olympus, Tokyo, Japan) equipped with differential interference contrast (DIC) and fluorescence optics (mirror units: U-FUNA: EX360-370, DM410, EM420-460; U-FBW: EX460-495, DM505, EM510IF; U-FGW: EX530-550, DM570, EM575IF (all Olympus), and Cy5: EX620/60, DM660, EM700/75 (Chroma, Irvine, CA, USA)). Images were acquired with Hamamatsu Orca R2 CCD camera (Hamamatsu

Photonics, Hamamatsu, Japan) and CellSens software (Olympus). Objectives used were:

1. 10x 0.3 numerical aperture (NA) air,
2. 20x 0.5 NA air, and
3. 40x 1.4 NA oil immersion.

For each image, the Z-stack option was used, making 10-20 slices per image, with slice spacings recommended by the software - 2 μm (10x objective), 1.27 μm (20x objective) and 0.35 μm (40x objective). Software used for image processing and analysis were CellSens and ImageJ by W. Rasband (U.S. National Institute of Health).

3.4. Gene silencing

The Fuse-It-siRNA (Beniag, Jülich, Germany) transfection kit was used to introduce specific small interfering ribonucleic acid (siRNA) molecules into the cells of the primary cortical cell cultures. Cells were transfected with one of the three different siRNAs specific to ATF3 (Table 4, all from Eurogentec, Seraing, Belgium).

Table 4 ***ATF3-specific siRNAs used in this work.***

ATF3-specific siRNA	sequence
S1	5’-GGAACCUCUUUAUCCAACA-3’
S2	5’-GUUGGAAAGUGUGAAUGCU-3’
S3	5’-AGAGACGAAGGGAAAGAAA-3’

A commercial siRNA specific to human beta actin (ACTB, SR-CL004-005, Eurogentec) 5’-UGAAGAUCAAGAUCAUUGC-3’ was used as a positive control for the transfection. A negative control siRNA (SR-CL000-005, Eurogentec) was used to demonstrate that the transfection does not induce

nonspecific effects on gene expression. Control siRNA (Fluorescein Conjugate)-A (sc-36869, SCBT) was used to visualize siRNA molecules in the cells after the transfection. The experimental setup was based on the manufacturer's instructions, with some modifications. Briefly, 10 µM siRNA was neutralized with Neutralization Buffer (NB, Beniag) for 10 min at RT, in a 1:2 volume ratio. Meanwhile, Fusogenic Solution (FS, Beniag) was sonicated in a precooled (4°C) ultrasonic bath for 5 min[3]. The amount of FS depended on the surface area of the cell culture, 1.25 µL and 5 µL per well for 24- and 6-well plate, respectively. FS was added to the neutralized siRNA solution, and again sonicated. This solution, undiluted transfection reagent, had to be diluted in neuronal medium (see 3.2.2.) to a volume sufficient to cover the whole well surface. The final volumes were 300 µL and 1 mL for 24- and 6-well plate, respectively. Prior to transfection, medium was removed from the cells and saved for later in a sterile Falcon tube. Half of the medium was replaced with fresh neuronal medium. Cells were washed two times with PBS at RT. Diluted and sonicated transfection reagent was then added to the cells and incubated for 15 min at 32°C. Transfection reagent was removed, and medium was added back to the cells. Cell cultures were maintained under the previously described conditions (see 3.2.2.). For gene silencing at the mRNA level, cells were treated after 1 day *in vitro* (DIV1) and harvested at DIV2. For gene silencing at the protein level, cells were treated at DIV1 and DIV2, and harvested at DIV3. Before harvesting, cells were imaged with a Zeiss inverted microscope (Zeiss, Jena, Germany) to check if transfection affected their morphology and/or viability. Transfection efficiency on the mRNA level was checked with RT-qPCR analysis, while that on the protein level was checked via Western blot.

[3] Each later sonication was performed under the same conditions.

3.5. Cell harvesting and sample preparation

Before detachment, cells were washed twice in PBS and incubated with prewarmed (32°C) 0.5% w/v trypsin for 5 min at 32°C. DMEM supplemented with 10% FBS was added to inactivate the reaction. Cells were centrifuged at 150 x *g* for 5 min at 4°C and the supernatant was discarded. Tubes containing cell pellets were immediately placed on ice. Either the RNA was immediately isolated, or the cell pellets were stored at -80°C for further analysis. For protein extraction, 2x Laemmli Sample Buffer (LSB, 20% w/v glycerol, 125 mM Tris HCl pH 6.8, 4% w/v sodium dodecyl sulphate (SDS), 0.2 M dithiothreitol, 0.02% bromophenol blue, all from Sigma-Aldrich) was added to the cell pellet, resuspended and briefly vortexed. The mixture was sonicated on ice with an ultrasonic homogenizer (SONOPULS mini20, BANDELIN electronic, Berlin, Germany) at the 20% amplitude 3x for 1 s. If not immediately used for gel-electrophoresis, samples were stored at -20°C.

3.6. Quantitative real-time PCR

3.6.1. RNA isolation

Total RNA was isolated from the cells using the Monarch Total RNA Miniprep kit (New England Biolabs (NEB), MA, USA) according to the manufacturer's instructions. It is a method of RNA purification that uses silica-based RNA capture columns. Briefly, samples were lysed with 300 µL of Lysis buffer and most of the genomic DNA (gDNA) was eliminated by centrifuging the sample through a gDNA removal column (NEB). RNA was then bound to the RNA purification column, washed, and treated with DNase I (NEB) for 15 min to additionally eliminate genomic DNA. RNA on the column was washed a few times and then eluted in 30 µL of nuclease-free water. Additional centrifugation was performed after elution and only the supernatant, containing isolated total RNA, was kept. All centrifugations were done at 16000 x *g* and all steps were performed at RT. The concentration and purity of the isolated RNA were assessed with a BioDrop

DUO spectrophotometer (Harvard Bioscience, Holliston, MA, USA). Absorbance ratio values at 260 nm and 230 nm ($A_{260/230}$), and at 260 nm and 280 nm ($A_{260/280}$) were measured. Ratios were considered acceptable when the $A_{260/230}$ was above 1.8 and the $A_{260/280}$ was about 2.2, which indicated that isolated RNA was of high purity. RNA quality was analyzed on a 1% agarose gel (Sigma-Aldrich) stained with SYBR Safe DNA Gel Stain (Thermo Fisher Scientific). 5 µL of RNA was mixed with 1 µL of Gel Loading Dye, Purple (6x, NEB) and loaded on the gel. Electrophoresis was performed at 75 V for 60 min, and gel was imaged with a ChemiDoc MP Imaging System (Bio-Rad, Hercules, CA, USA).

3.6.2. Reverse transcription

Isolated total RNA was reversely transcribed into complementary DNA (cDNA) with the ProtoScript II First Strand cDNA Synthesis Kit (NEB) following manufacturer's instructions for Standard Protocol (Table 5). Up to 1 µg of RNA was used in a 20 µL reaction. Sample RNA and Random Primer Mix (NEB) were denatured for 5 min at 65°C and cooled at 4°C until other components were added to the reaction. cDNA synthesis reaction was done at 42°C for 1 h. Reverse transcriptase was inactivated for 5 min at 80°C. For RT-qPCR, resulting cDNA was diluted 1:10 in nuclease free water. Diluted cDNA samples were stored at -20°C.

Table 5 ***Components used in cDNA synthesis reaction and their quantities.***

Component	Volume
total RNA	1-6 µL (up to 1 µg)
Random Primer Mix	2 µL
ProtoScript® II Reaction Mix (2x)	10 µL
ProtoScript® II Enzyme Mix (10x)	2 µL
nuclease-free water	to a total volume of 20 µL

3.6.3. Primer design

Opossum transcript sequences were downloaded from the Ensembl database, release 104 (24). Primers specific for genes of interest were designed with the Primer3Plus (33) web tool, and the primer sequence specificity was checked using the NCBI Nucleotide BLAST tool[4]. Selected primers (Table 6) were custom synthesized. ACTB was synthesized by Metabion (Metabion, Planegg, Germany), while ATF3 P1, ATF3 P2 and GAPDH were synthesized by Eurogentec.

Table 6 ***Primers used in RT-qPCR reactions.***

gene	Forward primer (5′ → 3′)	Reverse primer (5′ → 3′)
ATF3 P1	AGTTTGCCCCTGAAGAGGATG	CCAACTTTTCTGATTCCTTCTGC
ATF3 P2	AAGGAAGAGCTGAGGTTTGC	ATCCTCTTCAGGGGCAAACTC
ACTB	CAGACATCAGGGTGTGATGG	GGGGTGTTGAAGGTCTCAAA
GAPDH	ATGCCCCAATGTTCGTGATG	GTCATGAGTCCTTCCACAATGC

Specificity of primers was verified in a standard, routine PCR amplification reaction with undiluted cDNA as a starting material, to verify the predicted size of the amplification product. One*Taq* Hot Start 2x Master Mix with Standard Buffer (NEB) components were used in a reaction (Table 7). PCR amplification products were run on a 2% agarose gel.

[4] https://www.ncbi.nlm.nih.gov/

Table 7 ***Components used in routine PCR for assessing primer specificity.***

Component	Volume
undiluted cDNA	variable (up to 1 µg)
10 µM forward primer	0.5 µL
10 µM reverse primer	0.5 µL
One*Taq*® Hot Start 2x Master Mix with Standard Buffer	12.5 µL
nuclease-free water	to a total volume of 25 µL

3.6.4. RT-qPCR

Luna Universal qPCR Master Mix (NEB) was used to perform quantitative real-time polymerase chain reaction (RT-qPCR). This master mix is based on SYBR Green I fluorescent dye that binds double-stranded DNA. The reaction was done using a LightCycler 480 (Roche Holding, Basel, Switzerland) system and related software. The RT-qPCR program steps with indicated temperatures and times are listed in Table 8. As a reference gene, glyceraldehyde-3-phosphate dehydrogenase (GAPDH) was used, with the cycle threshold (Ct) value between 16 and 21. The cut-off value for Ct was 35 cycles. mRNA expression levels for all genes of interest (GOI) were calculated as relative to the expression level of the reference gene, GAPDH. The equation $2^{(\text{Ct value of GAPDH}) - (\text{Ct value of GOI})}$ was used in the analysis to calculate the fold change of GOI relative to the GAPDH. Final results were normalized to the untreated control samples and presented as fold change. All samples were done in technical duplicates.

Table 8 ***Steps of the RT-qPCR.***

Step	Temperature (°C)	Time (s)	Number of cycles
preincubation	95	600	1
3-step amplification:			
denaturation	95	10	45
annealing	55	10	
extension	72	20	
melting:			
	95	10	1
	65	60	
	97	1	
cooling	40	30	1

3.7. Western blot

The gels prepared for electrophoresis were 4% SDS-polyacrylamide stacking gel and 12% SDS-polyacrylamide separation gel. Sample preparation for Western blot (WB) was described in 3.5. Following the sonication step, samples were denatured on a thermo block at 95°C for 5 min. Samples were briefly spun down before loading. Electrophoresis was performed at 90 V for the stacking gel and at 150 V for the separation gel. Proteins were transferred onto nitrocellulose membrane (GE Healthcare, Chicago, IL, USA) for 70 min at 100 V. Membranes were stained in Ponceau S (Carl Roth) to check the efficiency of protein transfer to the membrane. Membranes were washed in TBS-T (0.1% Tween 20 in Tris-buffered saline, pH 7.4, all from Sigma-Aldrich) and blocked in the 5% BSA solution in TBS-T for 1 h on a shaker at RT. Membranes were incubated for 72 h on a shaker at 4°C with primary antibody specific to ATF3 (SCBT, sc-518032 X, 1:500) diluted in 3% BSA in TBS-T. Membranes were washed in TBS-T 3x for 5 min at RT on a shaker[5]. Incubation with secondary antibody, horseradish

[5] each latter washing step was the same

peroxidase (HRP)-linked goat anti-mouse (7076, Cell Signaling Technology, CST, Danvers, MA, USA, RRID: AB_330924, 1:2000) diluted in 1% BSA in TBS-T, was performed for 1 h at RT on a shaker. After the washing step, the chemiluminescent reagent Liteablot Turbo (Euroclone, Diagnostica, Milan, Italy) was added to membranes and incubated for 1 min at RT. Membranes were imaged with ChemiDoc MP Imaging System. Next, membranes were immunolabeled with HRP-conjugated ACTB (Sigma-Aldrich, A3854, RRID: AB_262011, 1:5000) and loading control GAPDH (Proteintech, HRP-60004, Rosemont, IL, USA, RRID: AB_2737588, 1:5000) antibodies. Membranes were blocked in 5% powdered milk (PM, Carl Roth) in TBS-T for 1 h at RT on a shaker. GAPDH antibody diluted in 3% PM in TBS-T was incubated overnight at 4°C on a shaker. Next day, membranes were washed and incubated with HRP-linked goat anti-mouse secondary antibody. HRP-linked ACTB antibody diluted in 3% PM in TBS-T was incubated for 15 min at RT on a shaker. Membranes were lastly washed, incubated with chemiluminescent reagent, and imaged as described before.

3.8. Data analysis

Immunofluorescence results are obtained from at least three independent experiments, and they are presented as bar graph with mean ± standard deviation (SD). Results from gene silencing experiments are obtained from one P3-5 litter, and two P16-18 litters, and they are presented as a bar graph with mean. Image and data analysis was done using ImageJ (immunofluorescence, Western blot) and LightCycler software (RT-qPCR).

ImageJ was used in immunofluorescence and WB data analysis. For immunofluorescence results, ImageJ was used to count cells expressing different cellular markers and different combinations of markers. The ImageJ CellCounter plugin was used to count the cells.

Quantification of WB results was performed with Analyze Gels tool within ImageJ program. Briefly, optical densities (OD) of GAPDH and protein of interest (POI) bands were measured for each sample. Relative OD of POI was calculated as a ratio between OD of POI and OD of GAPDH. Finally, relative OD of POI in each sample was divided with relative OD of POI in untreated sample. Results were shown as bar graph with mean, since there was insufficient number of replicates to perform statistical analysis.

3.8.1. Statistics

Statistical analysis was performed with GraphPad Prism 8.4 (GraphPad Software Inc., La Jolla, CA, USA). To test the normality of data, depending on the number of values tested, either D'Agostino–Pearson, or Shapiro–Wilk normality test was used. Brown–Forsythe test was used to test the equality of variances. One-way ANOVA was used to compare three or more data groups when data followed a Gaussian distribution, and then the Holm–Šídák test was performed for multiple comparisons between data groups. Data groups with different variances that fail a normality test were compared using the Kruskal–Wallis test, followed by Dunn's test for multiple comparisons between data groups. Student's *t*-test was used to compare two normally distributed data groups with equal variances, and in case of unequal variances, Welch's *t*-test was used. The accepted level of significance was $p < 0.05$. $p < 0.001$ very significant ***, $0.001 < p \leq 0.01$ very significant **, $0.01 < p < 0.05$ significant *, ≥ 0.05 not significant (ns).

4. RESULTS

4.1. Characterization of primary cortical cell cultures derived from the opossum *Monodelphis domestica*, and validation of different cellular markers

Primary cortical cultures were prepared from opossums *Monodelphis domestica* of two developmentally different ages, P3-5 and P16-18, that can or cannot regenerate their spinal cord after injury, respectively.

In Petrović et al. (31) we published a part of the data presented in this work. Pie charts and graphs in Figures 5-8 represent the data collectively obtained by all of the authors of that publication.

4.1.1. Expression of different neuronal markers

After dissociation of cortical tissue, primary cortical cells survived well and attached successfully to the surface. One day following plating, growing neurites and growth cones (GCs) were observed. Cells were stained with the cytoskeletal neuronal marker TUJ1 to visualize the neurites (Figure 4A,B). GCs are structures rich in actin and to confirm their formation we used fluorescently labeled phalloidin, which is a toxin that binds filamentous (F)-actin (Figure 4A,C).

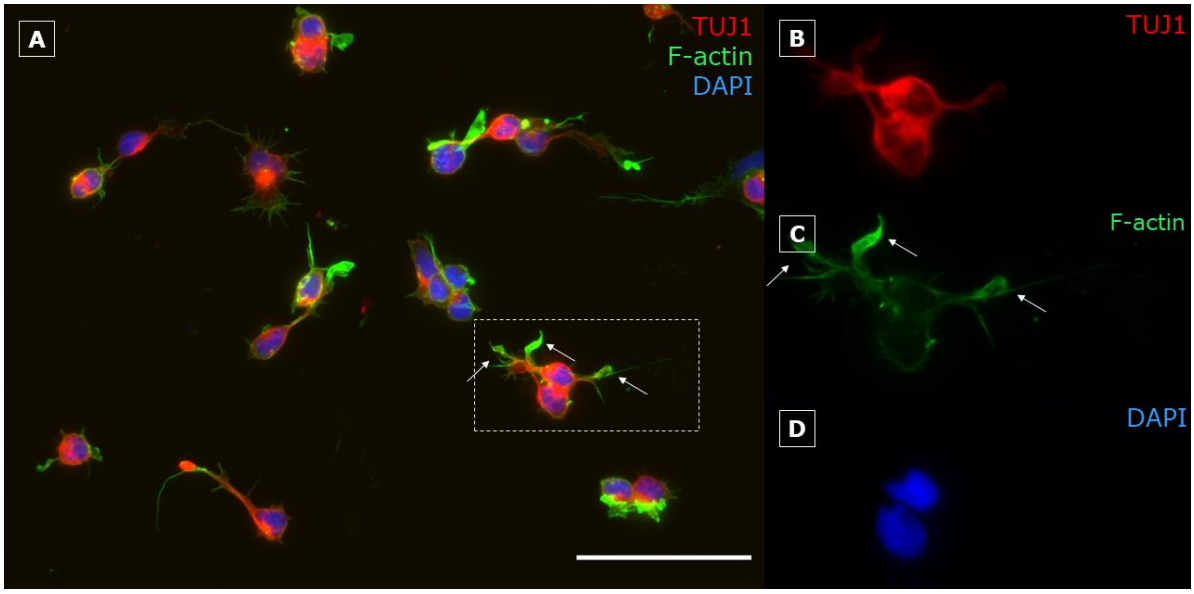

Figure 4 ***Developing neurons form growth cones (GCs) at the tips of growing neurites.*** *Cells derived from P5 opossums were fixed at DIV1 and stained for (B) β-tubulin III (TUJ1, red), (C) filamentous (F)-actin (green) and (D) nuclear stain DAPI (blue). (A) Merged image of all markers. Arrows indicate GCs. Scale bar, 50 µm.*

Cells in cultures from P3-5 opossums were comprehensively characterized using immunofluorescent microscopy. Cells were stained with antibodies for several neuronal markers, namely β-tubulin III (TUJ1), microtubule associated protein-2 (MAP2) and neuronal nuclei (NeuN).

At DIV1 (Figure 5), all the tested neuronal markers were detected in cultures. A majority of the cells (86.83 ± 2.20%, n = 367) stained triple positive for TUJ1, MAP2 and NeuN (TUJ1+/MAP2+/NeuN+). A smaller fraction of neurons (6.86 ± 1.70%, n = 367) expressed only NeuN (TUJ1-/MAP2-/NeuN+, Figure 5A-E, arrow) and there were also neurons (4.02 ± 1.90%, n =367) negative to TUJ1 (TUJ1-/MAP2+/NeuN+, Figure 5A-E, asterisk). The smallest proportion of cells (2.28 ± 0.78%, n =367) were triple negative non-neuronal cells (TUJ1-/MAP2-/NeuN-, Figure 5A-E, hash).

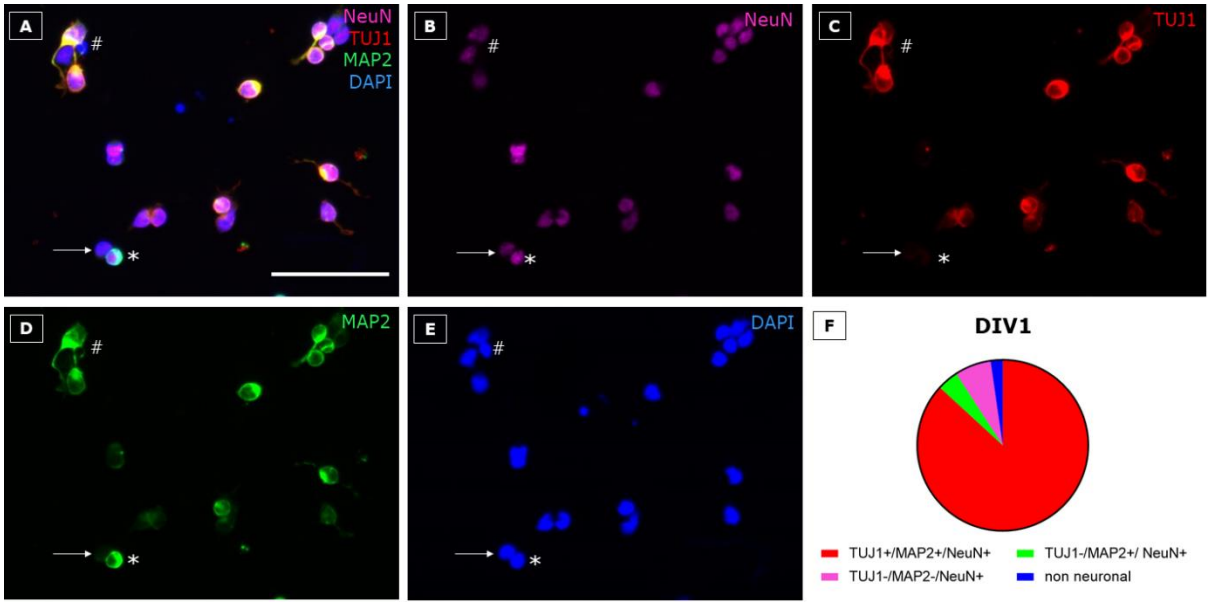

Figure 5 ***Primary cortical cells express neuronal markers at DIV1.*** *P3-5 opossum derived cortical cultures were fixed at DIV1 and stained for (B) neuronal nuclei (NeuN, magenta), (C) TUJ1 (red), (D) microtubule-associated protein-2 (MAP2, green), and (E) DAPI (blue). (A) Merged image of all markers. Asterisk indicates TUJ1-/MAP2+/NeuN+ cell, arrow indicates TUJ1-/MAP2-/NeuN+ cell, and hash indicates non-neuronal cell (TUJ1-/MAP2-/NeuN-). Scale bars, 50 µm. (F) Percentage of expression of TUJ1, MAP2 and NeuN at DIV1.*

At DIV4 (Figure 6), almost all (>97%) cells in our cultures were neurons. Most of them (93.11 ± 2.49%, n = 442) were triple positive (TUJ1+/MAP2+/NeuN+), others (4.53 ± 1.34%, n = 442) were positive only for NeuN (TUJ1-/MAP2-/NeuN+, Figure 6A-E, arrow) and numbers of TUJ1- neurons (TUJ1-/MAP2+/NeuN+, Figure 6A-E, asterisk) and non-neuronal cells (TUJ1-/MAP2-/NeuN-, Figure 6A-E, hash) were reduced (0.26 ± 0.64% and 2.11 ± 1.18%, respectively, n = 442), when compared to DIV1.

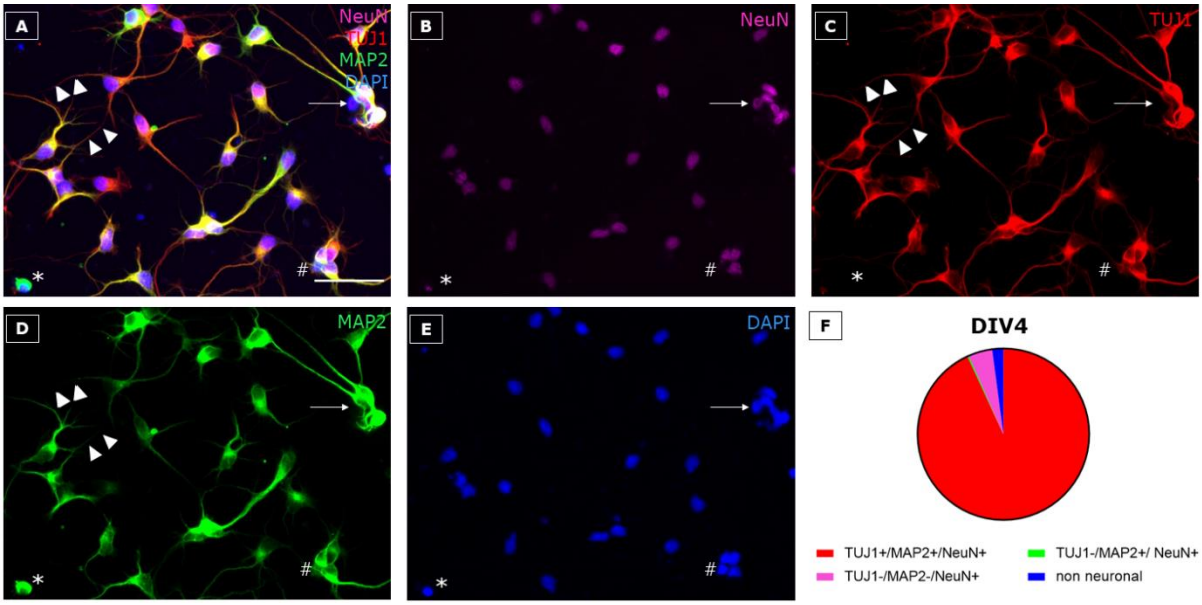

Figure 6 ***Primary cortical cells express neuronal markers at DIV4.*** *P3-5 opossum derived cortical cultures were fixed at DIV4 and stained for (B) neuronal nuclei (NeuN, magenta), (C) β-tubulin III (TUJ1, red), (D) microtubule-associated protein-2 (MAP2, green), and (E) nuclear stain 4',6-diamidino-2-phenylindole (DAPI, blue). (A) Merged image of all markers. Asterisk indicates TUJ1-/MAP2+/NeuN+ cell, arrow indicates TUJ1-/MAP2-/NeuN+ cell, and hash indicates non-neuronal cell (TUJ1-/MAP2-/NeuN-). Arrowheads are placed alongside TUJ1+/MAP2- axons. Scale bars, 50 µm. (F) Percentage of expression of TUJ1, MAP2 and NeuN at DIV4.*

At DIV7 (Figure 7) there was a decrease in the number of triple positive cells (TUJ1+/MAP2+/NeuN+, 83.37 ± 4.13%, n = 201), while the number of neurons expressing only NeuN (TUJ1-/MAP2-/NeuN+, Figure 7A-E, arrow) increased accordingly (10.2 ± 5.99%, n = 201). An increase in TUJ1-negative neurons (TUJ1-/MAP2+/NeuN+, Figure 7A-E, asterisk) was also observed (3.23 ± 3.40%, n = 201). At this period, the highest proportion of non-neuronal cells (TUJ1-/MAP2-/NeuN-, Figure 7A-E, hash) was present in the cultures (3.38 ± 1.47%, n = 201).

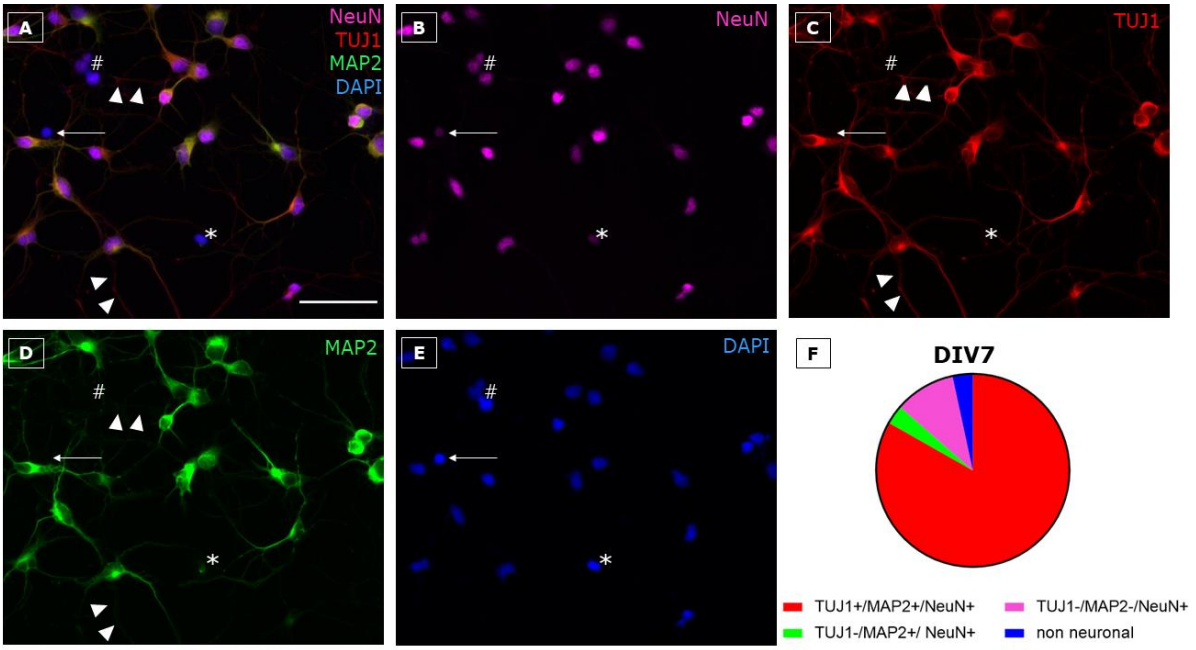

Figure 7 ***Primary cortical cells express neuronal markers at DIV7.*** *P3-5 opossum derived cortical cultures were fixed at DIV4 and stained for (B) neuronal nuclei (NeuN, magenta), (C) β-tubulin III (TUJ1, red), (D) microtubule-associated protein-2 (MAP2, green), and (E) nuclear stain 4',6-diamidino-2-phenylindole (DAPI, blue). (A) Merged image of all markers. Asterisk indicates TUJ1-/MAP2+/NeuN+ cell, arrow indicates TUJ1-/MAP2-/NeuN+ cell, and hash indicates non-neuronal cell (TUJ1-/MAP2-/NeuN-). Arrowheads are placed alongside TUJ1+/MAP2- axons. Scale bars, 50 μm. (F) Percentage of expression of TUJ1, MAP2 and NeuN at DIV7.*

The distribution of neuronal marker expression in different days *in vitro* is shown in pie charts (Figures 5-7F).

TUJ1 and MAP2 are both cytoskeletal markers in neurons, and they were used to observe the neurite outgrowth occurring *in vitro*. At DIV1, it was impossible to distinguish the axon from other neurites since all of them co-expressed TUJ1 and MAP2 (Figure 5). At DIV4 and DIV7, we were able to identify axons as TUJ1+/MAP2- neurites (Figures 6 and 7, arrowheads).

4.1.2. Primary neuronal cultures

After DIV1, primary cortical cultures derived from P3-5 opossums were maintained in neuronal medium (see Materials and Methods). Cultures mostly consisted of neurons, and the first connections were observed at DIV4. Neuronal networks formed over 3 weeks *in vitro* (Figure 8, upper

panel) and the percentage of TUJ1-positive neurons in the culture was evaluated for each time point analyzed (Figure 8G). Among all of the neuronal markers previously used, TUJ1 was the marker of choice because it stains neuronal soma, axons and dendrites, and thus, allowed the best visualization of neural networks. At DIV1 (Figure 8A), 84.82 ± 4.87% (n = 663) of cells were TUJ1+ neurons. The highest percentage of TUJ1+ neurons present in the culture occurred at DIV4 (92.66 ± 2.02%, n = 603), and it decreased afterwards. From DIV7 (Figure 8B) to DIV15 (Figure 8C), TUJ1+ neurons made up more than 80% of the culture (DIV7 86.28 ± 4.22%, n = 980, DIV11 83.28 ± 6.62%, n = 637, and DIV15 81.53 ± 8.46%, n = 560), but their number was significantly decreased at DIV22 (67.68 ± 8.46%, n = 633).

Network formation was also observed in cultures derived from P16-18 opossums (Figure 8, middle panel). Cells were maintained in neuronal medium for up to 3 weeks. Cells were fixed at DIV1, DIV7 and DIV15 (Figure 8D-F, respectively), stained for TUJ1 and counted (Figure 8H). The percentage of TUJ1+ neurons was lower compared to opossum P3-5 derived cultures. At DIV1, TUJ1+ neurons were 72.80 ± 19.24% of all cells in the culture (n = 2070, Figure 8D). At DIV7 this percentage increased to 82.37 ± 10.38% (n = 704, Figure 8E), and then it significantly decreased at DIV15 (55.59 ± 18.54%, n = 1514, Figure 8F).

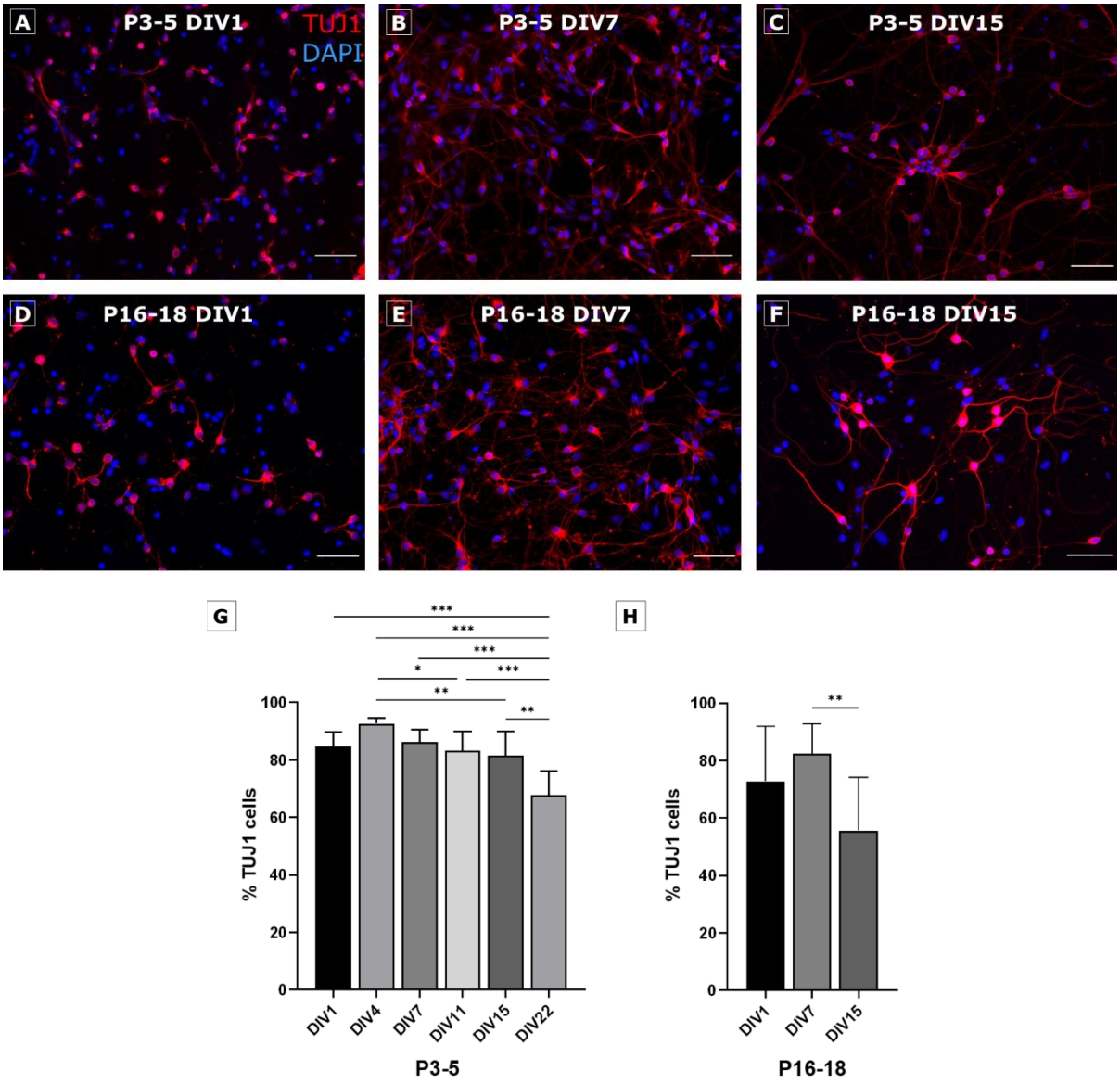

Figure 8 ***Development of neuronal networks in primary neuronal cultures.*** *Cells derived from P3-5 (top panel) and P16-18 (middle panel) opossums were fixed at (A, D) DIV1, (B, E) DIV7 and (C, F) DIV15. Samples were stained for TUJ1 (red) and nuclear stain DAPI (blue). Scale bars, 50 µm. (G) Histogram showing the percentage of neurons in P3-5 cultures at different times as indicated below the bars. One-way ANOVA followed with Holm–Šídák* post-hoc *test. DIV1 vs. DIV22 p < 0.001***, DIV4 vs. DIV11 p = 0.0395*, DIV4 vs. DIV15 p = 0.0064**, DIV4 vs. DIV22 p < 0.001***, DIV7 vs. DIV22 p < 0.001***, DIV15 vs. DIV22 p = 0.0013**. (H) Histogram showing the percentage of neurons in P16-18 cultures at different times as indicated below the bars. Kruskal-Wallis test followed with Dunn's* post-hoc *test. DIV7 vs. DIV15 p = 0.0071**.*

During the second week in culture, cell aggregates (Figure 9) started to form in cultures derived from opossums of both ages. These spherical aggregates consisted of clustered neuronal bodies, whose neurites spread radially from the aggregates.

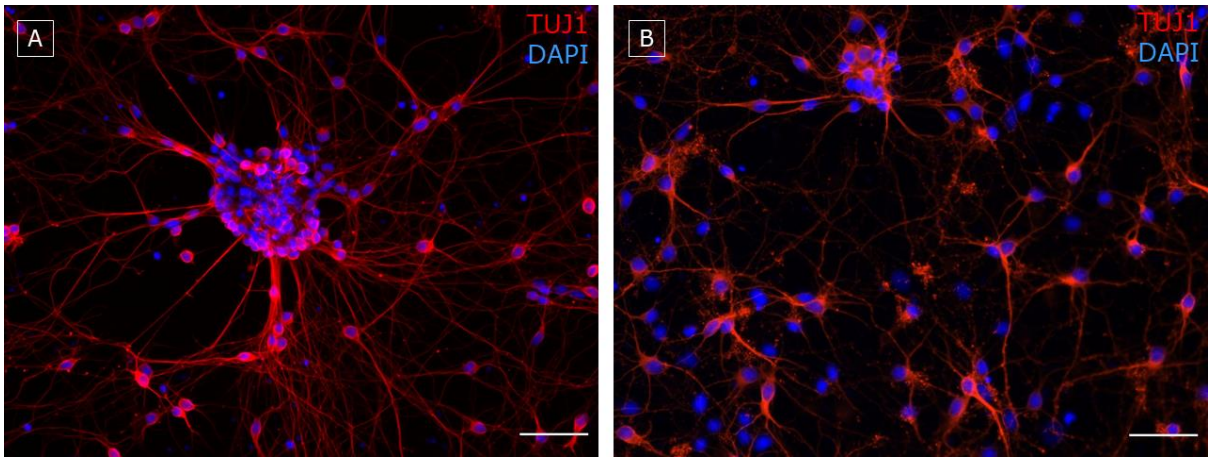

Figure 9 ***Primary neurons derived from opossums of both ages, P3-5 and P16-18, form aggregates*** **in vitro.** *Cells derived from (A) P3-5 and (B) P16-18 opossums were fixed at DIV15 and DIV7, respectively, and stained with anti-TUJ1 antibody (red) and nuclear stain DAPI (blue). Cells positive to TUJ1 of both ages formed aggregates and spread their neurites radially. Scale bars, 50 µm.*

4.1.3. Synapse formation

Cells were fixed at DIV15 when cell connections were abundant, and they were then stained for TUJ1 and synapsin I. Synapsin I is a presynaptic vesicle protein, and anti-synapsin I was previously used in opossum (34). It was confirmed that opossum-derived primary cortical neurons successfully form neuronal networks *in vitro* and that synapses are present at DIV15 (Figure 10) when the neuronal network is generally considered mature (35).

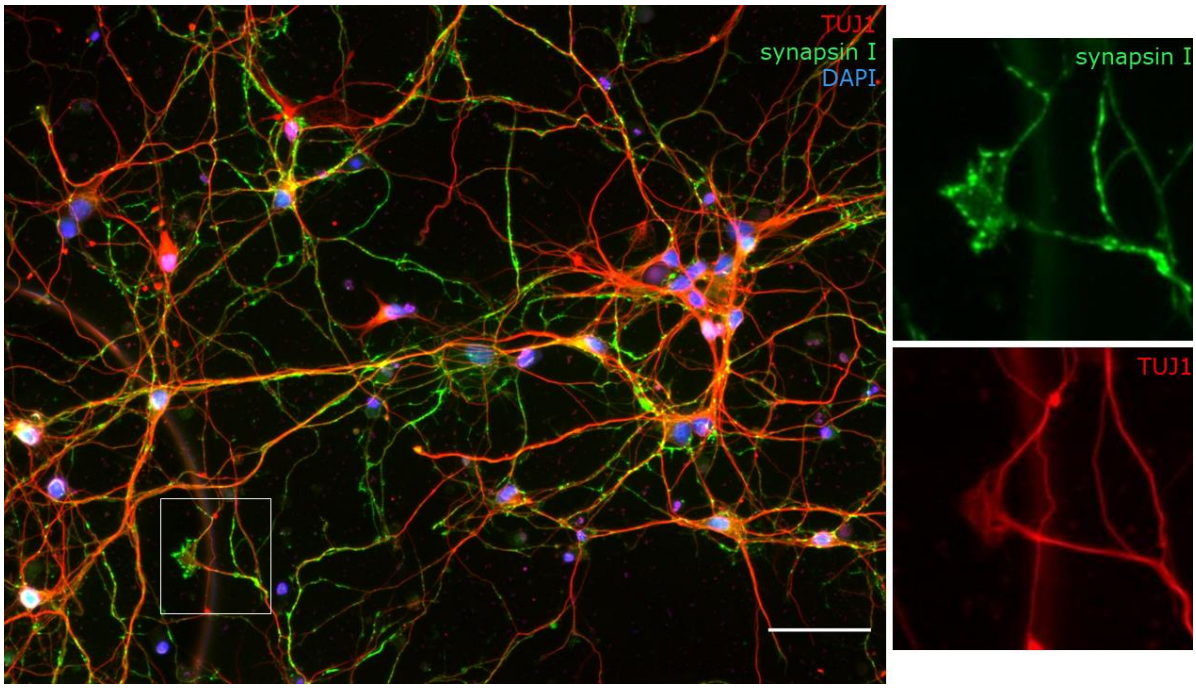

Figure 10 ***Primary cortical neurons form synapses*** **in vitro.** *P5 opossum derived cortical cultures were fixed at DIV15 and stained for TUJ1 (red), synapsin I (green) and nuclear stain DAPI (blue). For better visualization of stained synapses, part of the image marked with white square is shown enlarged in the right panels, separately for (top panel) synapsin I and (bottom panel) TUJ1 staining. Scale bar, 50 μm.*

4.1.4. Proliferative cells

Opossum brain development continues postnatally, and it was therefore assumed that the proliferative progenitor/radial glial cells would be present in primary cortical cell cultures.

To evaluate the proliferation capacity of the cells, a proliferation assay was performed using the Click-iT EdU Proliferation Kit (Figure 11). In the first experiment, following fixation, cells were stained for vimentin and GFAP to investigate whether proliferative cells (EdU+) express glial markers (Figure 11A-D). In the second experiment, cells were stained for TUJ1 (Figure 11E-G) to confirm that cells that express neuronal markers are not proliferative.

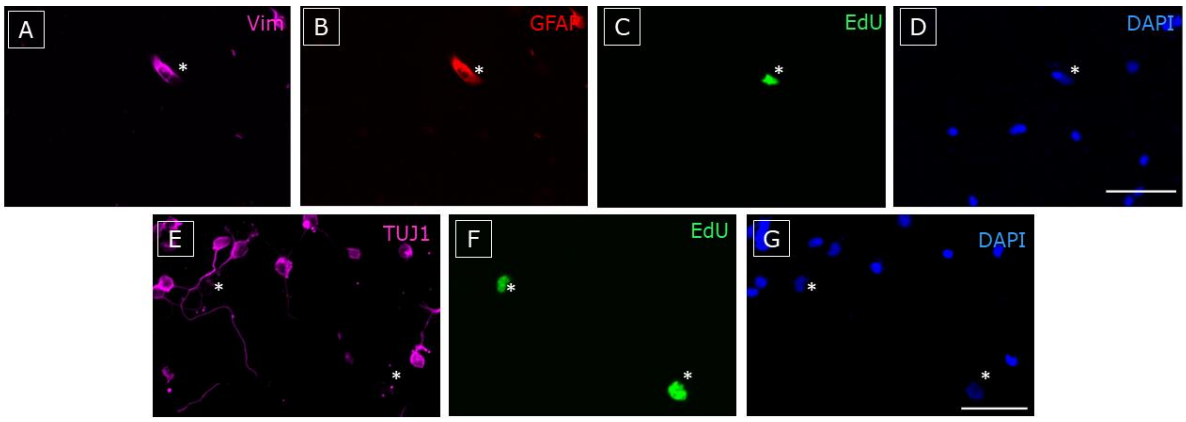

Figure 11 ***Primary cortical cultures contain proliferative cells.*** *Two P3-5 cultures (A-D and E-G) were tested for proliferation with Click-iT EdU Proliferation Kit at DIV1 and fixed at DIV2. Cells were stained for (A) vimentin (Vim, magenta), (B) GFAP (red), (C, F) EdU (see Materials and Methods, green), (D, G) nuclear stain DAPI (blue) and (E) TUJ1 (magenta). Asterisks indicate proliferative cells (EdU+) positive for vimentin and/or GFAP in upper panel, and negative to TUJ1 in lower panel. Scale bars, 50 μm.*

In addition, it was examined whether the proliferative characteristic of cells is preserved *in vitro*. To sustain proliferation, cells were maintained in proliferative medium containing serum. Specifically, proliferative medium consisted of DMEM with stable glutamine supplemented with 10% w/v FBS (see Materials and Methods). The number of proliferative cells (EdU+) was counted at DIV1 and DIV7 (Figure 12). The percentage of EdU+

cells was expected to increase as proliferative cells would have to divide and therefore increase their number. At DIV1, EdU+ cells were 18.15 ± 5.36% (n = 575, Figure 12A,C) of the total number of cells, while, as expected, at DIV7 their number increased significantly to 57.70 ± 15.42% (n = 740, Figure 12B,C).

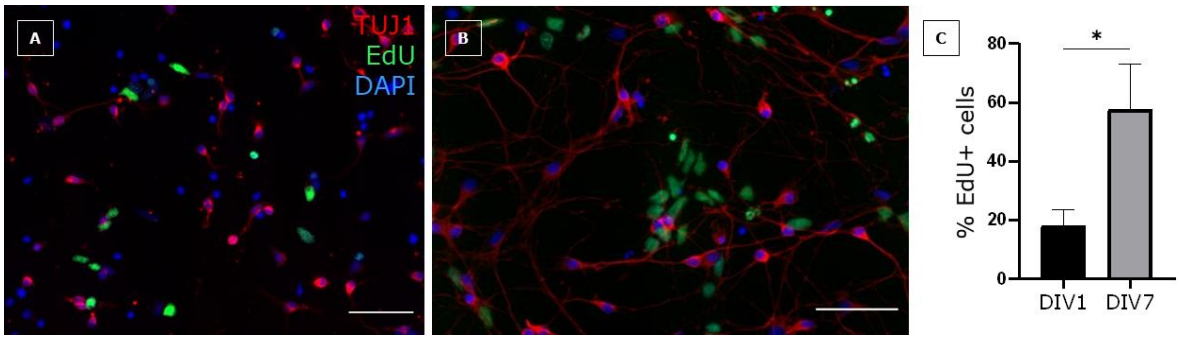

Figure 12 ***Cells can be maintained in a proliferative state using the proliferative medium.*** *Opossum P3-5 derived primary cortical cultures were maintained in proliferative medium (see Materials and Methods) and fixed at (A) DIV1 and (B) DIV7. Click-iT EdU was added to the cells 24 h prior to fixation. Cells were stained for TUJ1 (red), EdU (green) and nuclear stain DAPI (blue). Scale bar, 50 µm. (C) Histogram showing the percentage of EdU+ cells at DIV1 and DIV7. Unpaired* t*-test with Welch's correction. DIV1 vs. DIV7 p = 0.0418*.*

It was hypothesized that the proliferative cells seen in primary cortical cell cultures could be radial glial cells (RGCs). Previous experiments demonstrated that proliferative cells express vimentin and GFAP. However, Vim+/EdU+ cells could instead be fibroblasts from meningeal tissue, and GFAP+/EdU+ cells could instead be astrocytes. Figure 9 shows a triple positive GFAP+/Vim+/EdU+ cell, implying that cortical cultures contain RGCs. Therefore, to be more accurate in RGC characterization, cells were double stained for Pax6 and vimentin, and it was observed that all Vim+ cells are positive to Pax6 (Figure 13).

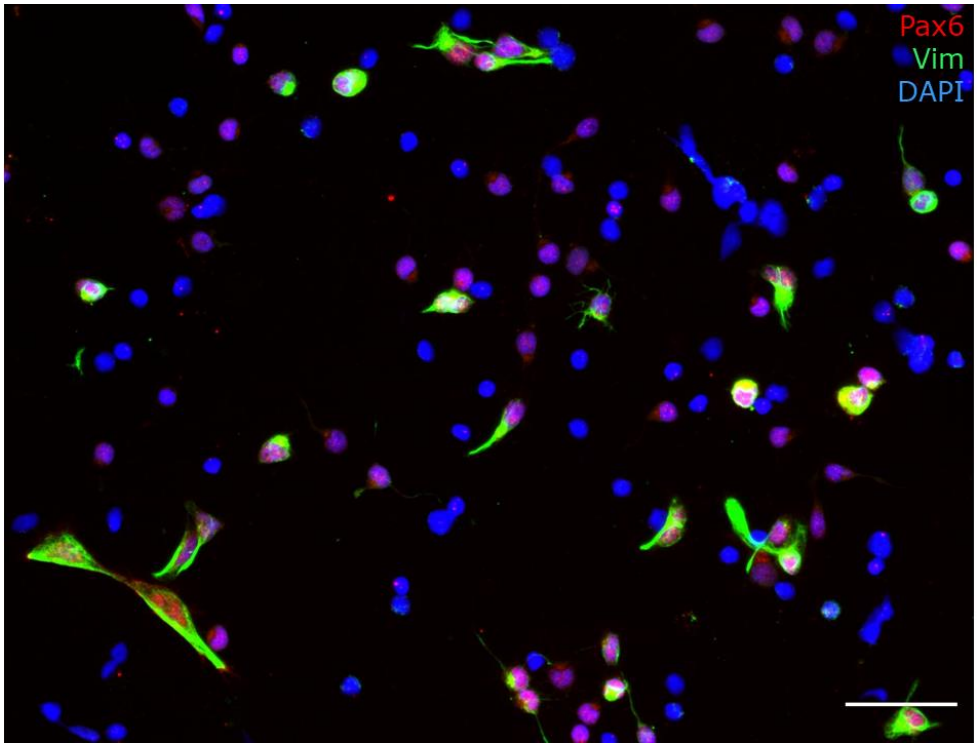

Figure 13 ***Cortical radial glial cells express Pax6 and vimentin.*** *P3-5 culture was fixed at DIV1 and stained for paired box-6 transcription factor (Pax6, red), vimentin (Vim, green) and nuclear stain DAPI (blue). Scale bar, 50 μm.*

4.2. Gene silencing

In order to confirm that primary cortical cell cultures derived from *Monodelphis domestica* can be used as a model in the postnatal CNS regeneration research, a gene silencing protocol was optimized.

4.2.1. siRNA transfection protocol optimization

A novel siRNA transfection protocol was established because this technique has never been used before in primary cortical cell cultures derived from *Monodelphis domestica*. Following successful characterization of primary cortical cell cultures, these cells were used in gene silencing experiments. The transfection method was based on the fusion of a liposomal carrier with a cell membrane.

Firstly, the cells were treated with a transfection reagent containing the fluorescein-conjugated siRNA (Figure 14). Transfection was performed

according to the manufacturer's instructions. Fluorescently labelled siRNA enabled visualization of the transfected cells under the fluorescent microscope. siRNA successfully entered the cells, and transfected cells were alive for at least 4 h after transfection (Figure 14).

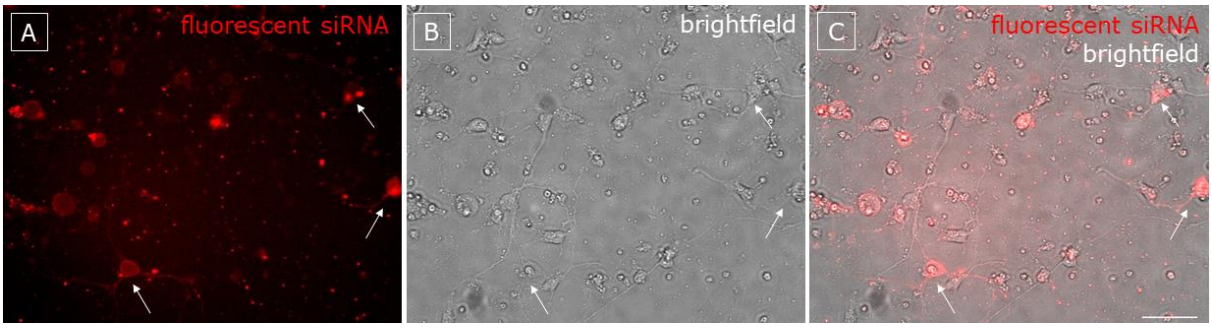

Figure 14 ***Transfection reagent successfully delivers siRNA into the cells.*** *P5 cultures were transfected at DIV7 with fluorescent siRNA and imaged after 4h using the (A) fluorescent and (B) brightfield microscopy. (C) Merged image of (A) and (B). Scale bar, 50 µm.*

In the optimization process, cells were targeted with siRNA specific to actin beta (ACTB siRNA). ACTB siRNA is a commercially available positive control for siRNA knockdown experiments, and it is specific for human actin beta (hACTB). Its sequence was compared to the predicted opossum ACTB sequence (Figure 15) available in the Ensembl database. Alignment was performed using the Multiple Sequence Alignment tool within Clustal Omega web application (36). ACTB siRNA was used in the optimization phase despite the observed difference.

```
opossum     GGTGGTACCACCATGTACCCAGGCATTGCTGACAGGATGCAGAAGGAGATTACAGCCCTA
siRNA       ------------------------------------------------------------

                                  ↓
opossum     GCCCCCAGCACAATGAAAATCAAGATCATTGCCCCACCTGAGCGCAAATACTCTGTCTGG
siRNA       -------------TGAAGATCAAGATCATTGC----------------------------
                        **** **************

opossum     ATTGGAGGCTCCATCCTGGCCTCCCTCTCCACCTTCCAACAGATGTGGATCAGTAAGCAG
siRNA       ------------------------------------------------------------
```

Figure 15 ***A single nucleotide mismatch between commercially available ACTB siRNA and siRNA-binding site on the predicted opossum ACTB gene sequence.*** *Aligned nucleotides are marked with asterisks. There is one mismatch (arrow) at the position 5 of the ACTB siRNA.*

To investigate whether the transfection procedure would affect the cell viability, P5 cells cultured in a 24-well plate were treated at DIV1 (Figure 16). One set of the cells was left untreated (Figure 16A) and other cells were treated either with the siRNA-free transfection reagent (Figure 16B) or transfection reagent containing 10 pmol ACTB siRNA (Figure 16C). siRNA-free transfection reagent was added to one set of the cells (vehicle-treated) to test the effect of the reagent itself on cell viability. Cells were treated for 15 minutes and then immediately imaged.

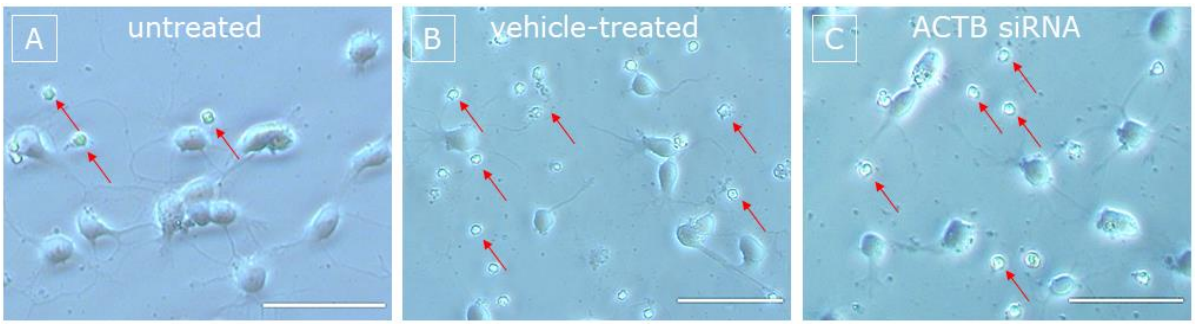

Figure 16 ***Cell survival after transfection.*** *(A) Untreated P5 cells at DIV1. Other cells were treated at DIV1 with either (B) siRNA-free transfection reagent or (C) transfection reagent containing ACTB siRNA. Cells were imaged with phase contrast immediately after treatment. Arrows indicate dead cells. Scale bars, 50 µm.*

Next, the transfection was performed in the P5 culture at DIV7 (Figure 17). Different concentrations of ACTB siRNA (10 pmol and 20 pmol) and incubation times (15 min, 30 min, 45 min and 60 min) were tested. 20 pmol of siRNA was lethal to the cells at all indicated incubation times. When 10 pmol of siRNA was used, more cells died with increasing incubation time. For further transfections performed in a 24-well plate, 10 pmol of siRNA per well was incubated with cells for 15 min at 32°C.

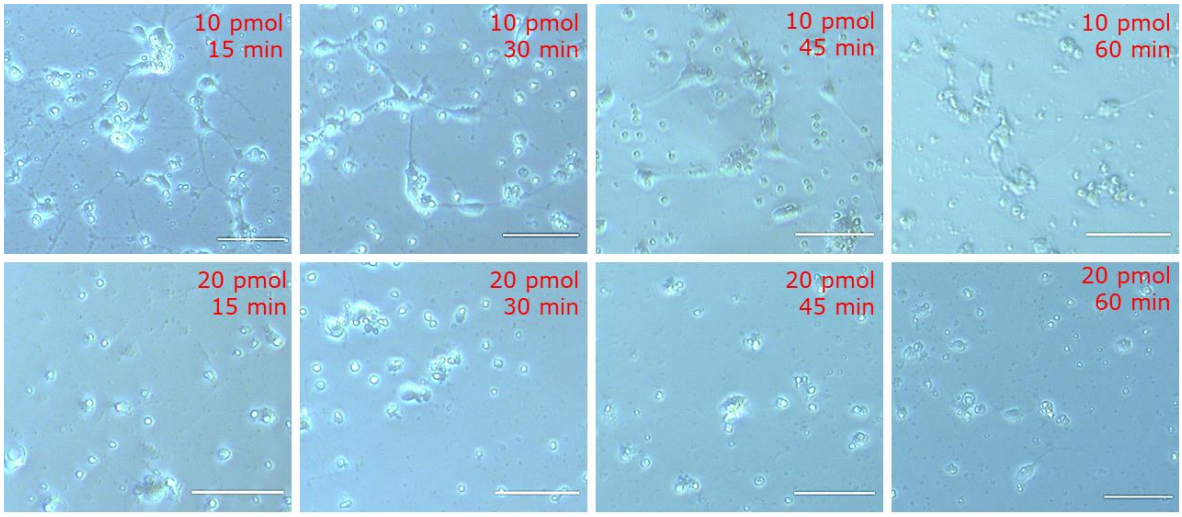

Figure 17 ***For transfection of cells cultured in a 24-well plate, optimal siRNA concentration is 10 pmol/well and optimal incubation time is 15 min.*** *P5 culture was transfected with ACTB siRNA at DIV7 to test different siRNA concentrations and incubation times. siRNA concentrations and incubation times are indicated in upper right corner of each image. Cells were imaged with phase-contrast immediately after treatment. Scale bars, 50 µm.*

Furthermore, to optimize the amount of siRNA needed for silencing on a larger scale, P18 cells were plated in 6-well plates and transfected with 30 or 60 pmol of ACTB siRNA per well at DIV1 (Figure 18). The incubation time was 15 min. A higher concentration of siRNA (60 pmol) was toxic to the cells, and therefore, 30 pmol of siRNA per well was used for further transfections.

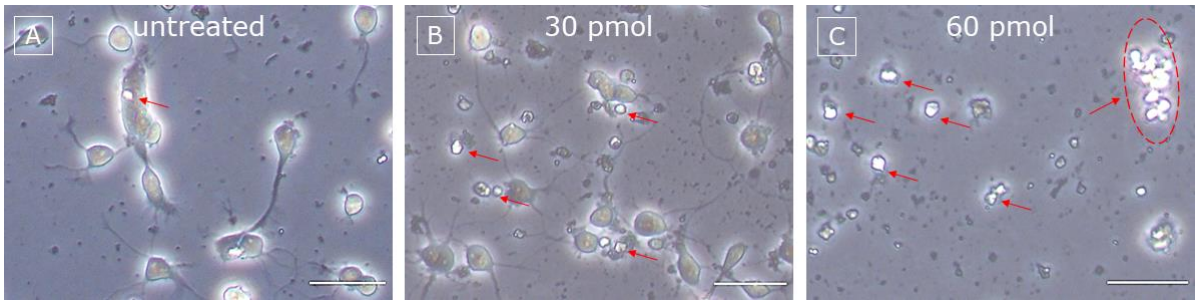

Figure 18 ***In a 6-well plate, optimal siRNA concentration is 30 pmol/well.*** *P18 cells at DIV2. Cells were (A) untreated or transfected at DIV1 with either (B) 30 or (C) 60 pmol of ACTB siRNA per well. Amount of siRNA used per well is indicated. Arrows indicate dead cells. Notice the aggregate of dead cells in the sample transfected with 60 pmol of ACTB siRNA, in the red oval. Scale bars, 50 µm.*

In the final optimization step, to improve the cell viability, it was assessed whether it was better to dilute the transfection reagent in PBS or neuronal medium. P5 cells were cultured in a 6-well plate and transfected at DIV1 with transfection reagent diluted either in PBS or neuronal medium (NB/B27), and one set of cells were left untreated. Next day, cells were imaged (Figure 19, upper panel) and harvested. The highest concentration of total RNA was isolated from untreated cells (c = 38.77 ng/μL), while in two other samples the concentration was lower (PBS c = 22.89 ng/μL, NB/B27 c = 23.88 ng/μL, Figure 19A). Agarose gel electrophoresis confirmed good quality of isolated total RNA (Figure 19A). The RNA was reversely transcribed into cDNA, and cDNA from untreated cells was used to test the specificity of ACTB and GAPDH primers (Figure 19B) designed for RT-qPCR analysis. After RT-qPCR, it was calculated that mRNA expression of ACTB was reduced by 11.73% when the transfection reagent was diluted in PBS, and when the transfection reagent was diluted in neuronal medium, ACTB expression reduced by 53.02% (Figure 19B). In WB analysis, a membrane was immunolabeled with ACTB and GAPDH antibodies (Figure 19C). Expression of ACTB was decreased in both transfected samples. When transfection reagent was diluted in PBS, ACTB expression was reduced by 35.65%, and when transfection reagent was diluted in neuronal medium, ACTB expression was reduced by 33.79% (Figure 19C).

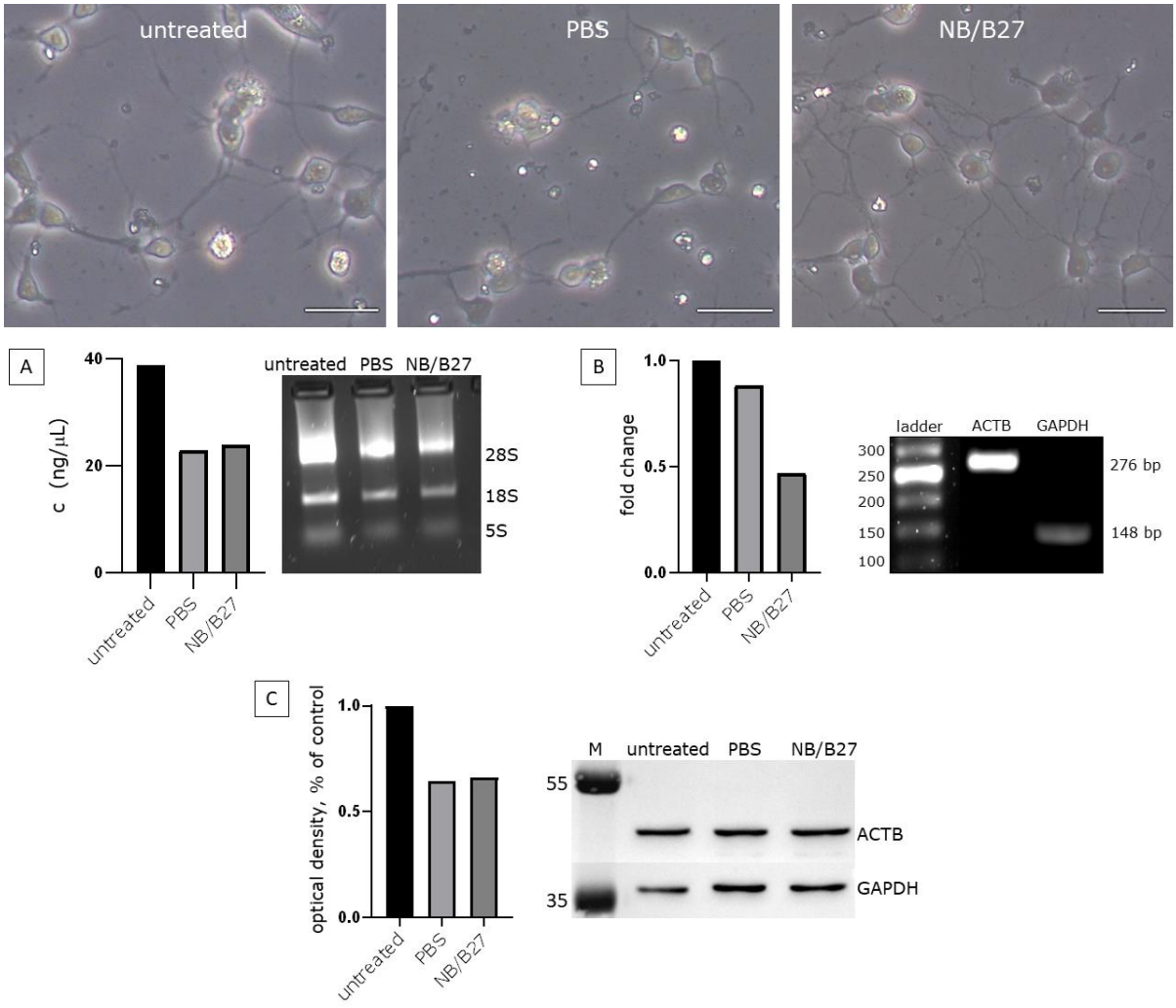

Figure 19 ***Transfection is more efficient on mRNA level when transfection reagent is diluted in neuronal medium.*** *P5 cells were imaged with phase contrast at DIV2 (upper panel). Part of the cells was treated at DIV1 with ACTB siRNA diluted in either PBS or neuronal medium (NB/B27). Scale bars, 50 µm. (A) Bar graph showing concentrations of total RNA isolated from P5 cells at DIV2. Quality of total RNA was assessed on 1% agarose gel. (B) RT-qPCR. ACTB mRNA levels were normalized to GAPDH mRNA levels. Bar graph showing fold change of ACTB expression in treated samples compared to untreated control. 2% agarose gel electrophoresis of endpoint RT-PCR products. PCR product sizes are indicated on the right. (C) Western blot. Bar graph showing relative change of ACTB protein levels in treated samples, compared to untreated sample. GAPDH was a loading control.*

4.2.2. Alignment of the human and opossum ATF3 isoforms

Alignment of human and opossum ATF3 protein amino sequences using the Clustal Omega[6] web tool (Figure 20) showed that their amino acid sequences are 92.27% identical and that all possible PTM sites from human ATF3 are conserved in opossum. PTM sites are Lys78, Lys175 (SUMOylation, Figure 20, red boxes), and Thr162 (phosphorylation, Figure 20, blue box).

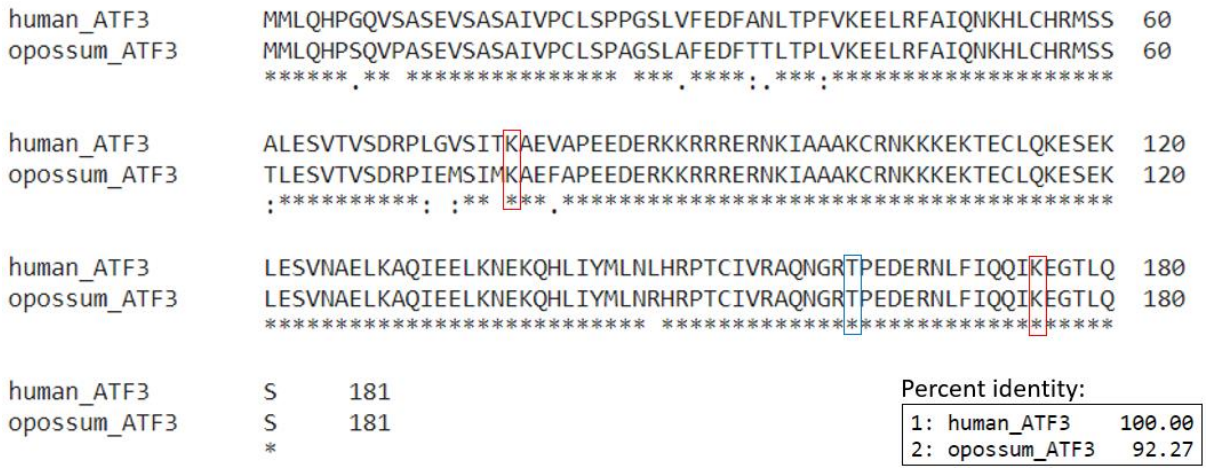

Figure 20 ***Posttranslational modification sites defined for human ATF3 are conserved in opossum ATF3.*** *Clustal alignment of human and opossum ATF3 amino acid sequences. Red boxes indicate SUMOylation sites, while blue box indicates phosphorylation site.*

Additionally, alignment of human and opossum ATF3ΔZip amino acid sequences was performed (Figure 21). In human ATF3ΔZip there is one PTM site detected, SUMOylation at Lys78, and it is conserved in opossum ATF3ΔZip (Figure 21, red box). Human and opossum ATF3ΔZip amino acid sequences are 86.44% identical.

[6] https://www.ebi.ac.uk/Tools/msa/clustalo/

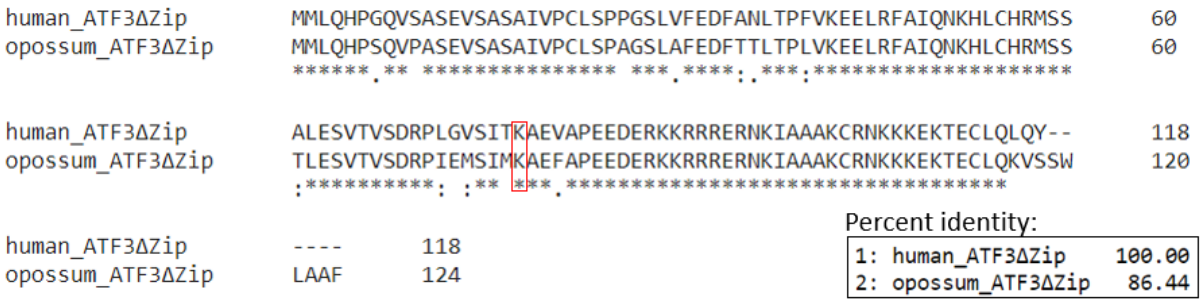

Figure 21 ***Posttranslational modification site defined for human ATF3ΔZip is conserved in opossum ATF3ΔZip.*** *Clustal alignment of human and opossum ATF3ΔZip amino acid sequences. Red box indicates SUMOylation site.*

4.2.3. Silencing of ATF3

Gene silencing of the activating transcription factor 3 (ATF3) was performed using siRNA molecules specific for the ATF3 mRNA sequence. ATF3 was selected as a gene of interest since it has a confirmed role in adult PNS regeneration (25,26).

All ATF3-specific siRNAs (S1, S2, S3) target the ATF3 transcript 201, while only S3 siRNA targets the ATF3 transcript 202. Two different primer pairs for ATF3 were used, since ATF3 gene codes for two known transcripts, ATF3 201 and ATF3 202 (24). ATF3 primer pair 1 (ATF3 P1) is specific for ATF3 201 transcript, and ATF3 primer pair 2 (ATF3 P2) amplifies both transcripts. For easier understanding, these claims are schematically presented (Figure 22).

siRNA

	ATF3 201 transcript	ATF3 202 transcript
ATF3 S1	✓	✖
ATF3 S2	✓	✖
ATF3 S3	✓	✓

primer pair

	ATF3 201 transcript	ATF3 202 transcript
ATF3 P1	✓	✖
ATF3 P2	✓	✓

Figure 22 ***Gene silencing experimental design.*** *Schematic overview of ATF3-specific siRNA (left table) and primer (right table) targets.*

ATF3 silencing experiments were performed once in primary cortical cultures derived from P3-5 opossums and twice in cultures derived from

P16-18 opossums. These preliminary results are analyzed and presented separately for each age, since the opossums of these two indicated ages are developmentally different and as such are presented throughout this work. The entire course of the experimental work was carried out as described in Materials and Methods.

RNA was isolated from P3-5 opossums derived cells, 35.20 ± 3.86 ng/µL total. The isolated RNA was pure, with $A_{260/230}$ and $A_{260/280}$ ratios of 2.507 ± 0.143 and 2.056 ± 0.032, respectively, and of good quality. RT-qPCR results indicate that ATF3 was successfully silenced at mRNA level in all samples treated with ATF3-specific siRNAs. In a sample transfected with ATF3 S1 siRNA, ATF3 201 transcript expression was reduced by 53.39% (Figure 23A), while the expression of both transcripts was 60.16% lower compared to the control sample (Figure 23B). In a sample transfected with ATF3 S2 siRNA, ATF3 201 transcript expression was reduced by 47.21% (Figure 23A), while the expression of both transcripts was 55.40% lower than in control sample (Figure 23B). In a sample transfected with ATF3 S3 siRNA, ATF3 201 transcript expression was reduced by 46.58% (Figure 23A), while the expression of both transcripts was 42.77% lower compared to the control sample (Figure 23B).

From cultures derived from P16-18 opossums, 66.31 ± 24.77 ng/µL total RNA was isolated. The isolated RNA was pure, with $A_{260/230}$ and $A_{260/280}$ ratios of 2.227 ± 0.232 and 2.123 ± 0.036, respectively, and of good quality. RT-qPCR was performed, and the results indicated a lower silencing efficiency than in P3-5 culture. In sample transfected with ATF3 S1 siRNA, ATF3 201 transcript expression was reduced by 8.47% (Figure 23D), while the expression of both transcripts was 6.12% lower than in control sample (Figure 23E). In a sample transfected with ATF3 S2 siRNA, ATF3 201 transcript expression was reduced by 10.76% (Figure 23D), while the expression of both transcripts was 16.26% lower compared to the control sample (Figure 23E). In a sample transfected with ATF3 S3 siRNA, ATF3 201 transcript expression was reduced by 5.01% (Figure 23D), while the

expression of both transcripts was 11.09% lower compared to the control sample (Figure 23E). In samples transfected with negative control siRNA, ATF3 mRNA levels of 201 and both 201 and 202 transcripts were 1.74% lower (Figure 23D) and 15.20% higher (Figure 23E) compared to the control sample, respectively.

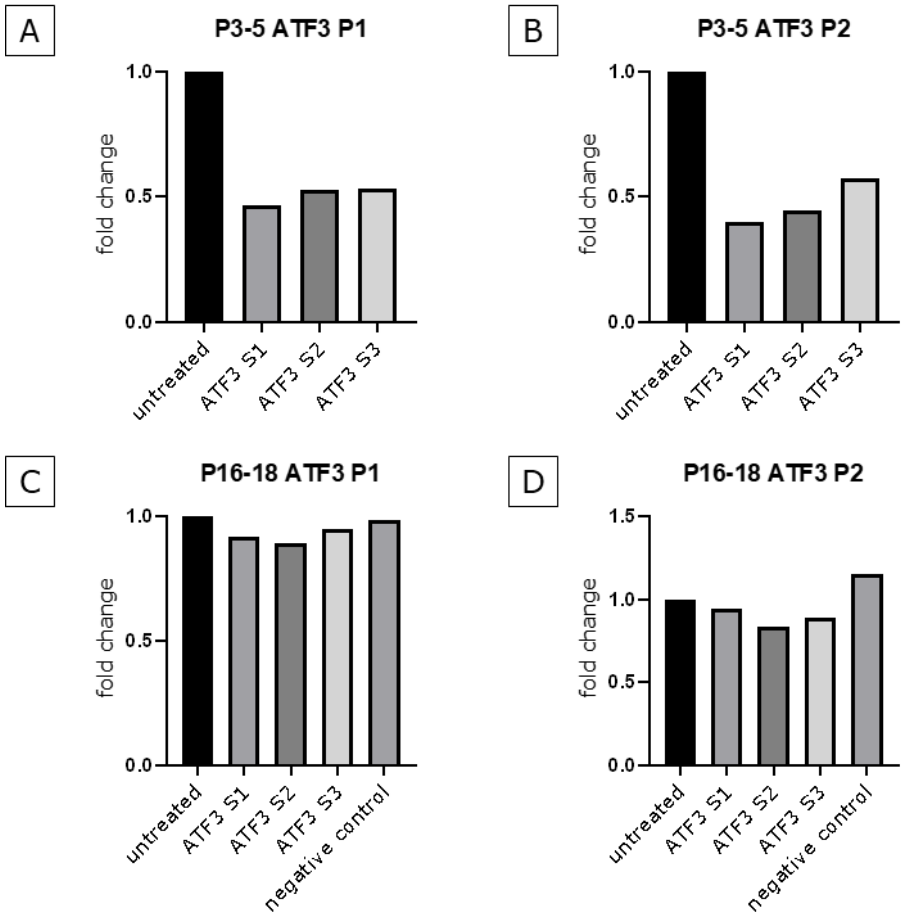

Figure 23 ***Silencing of ATF3 at mRNA level is more effective in P3-5 opossum cultures.*** *Transfection of (A,B) P3-5 and (C,D) P16-18 opossum primary cortical cultures with ATF3-specific siRNAs (S1, S2 and S3), and negative control siRNA was performed at DIV1. mRNA levels of ATF3 isoforms were assessed by RT-qPCR analysis. Data are calculated as mean and represented as bar graph. mRNA levels in treated samples are shown as fold change relative to the untreated sample. (A,C) ATF3 201 mRNA levels. (B,D) ATF3 201 and 202 mRNA levels.*

Other sets of samples from P3-5 and P16-18 cultures, that were transfected at DIV1 and DIV2, were lysed in 2x LSB and homogenized. To

determine silencing efficiency at the protein level, samples were analyzed as described in Materials and Methods.

From information available in the literature, the signal for ATF3 was expected at two different molecular weights, at 14 and 22 kDa. Interestingly, in P3-5 cultures there were three, and in P16-18 cultures there were five different bands detected after immunolabelling with an ATF3-specific antibody. An additional band in P3-5 cultures was detected at 25 kDa (Figure 24A), and in P16-18 cultures, two more isoforms were detected, at 30 and 35 kDa (Figure 25A).

In P3-5 cultures (Figure 24), 14 kDa isoform expression (Figure 24B) was decreased in samples treated with ATF3 specific siRNAs (S1 -34.62%, S2 -34.73% and S3 -49.18%). However, in negative control samples the expression was also reduced by 28.21%. 22 kDa isoform expression (Figure 24C) remained almost the same in samples treated with ATF3 S1 and S2 siRNAs, +2.50% and -0.13%, respectively, while in samples treated with ATF3 S3 siRNA the expression decreased by 39.44%. In negative control samples, the expression was 27.88% lower than in control samples. Expression of 25 kDa ATF3 form (Figure 24D) increased after treatment with ATF3 S1-3 siRNAs, +73.40%, +33.50% and +29.20%, respectively, and in negative control samples it remained unchanged (-4.46%).

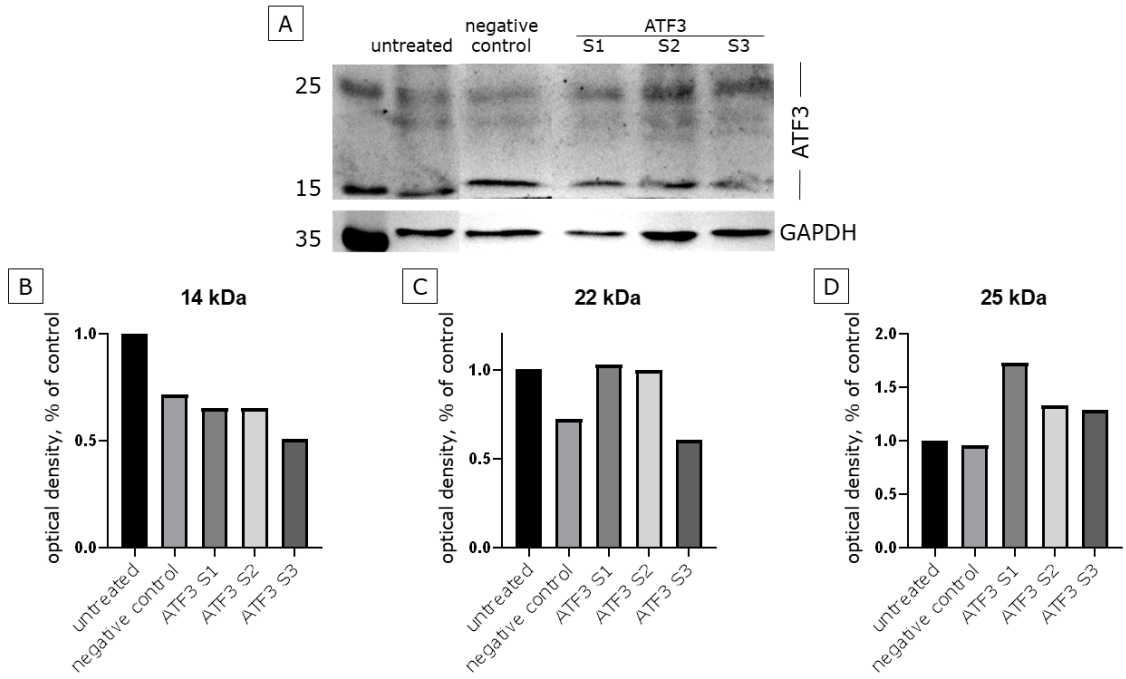

Figure 24 ***Expression levels of ATF3 (iso)forms in P3-5 cultures after silencing of ATF3.*** *P3-5 cultures were treated at DIV1 and DIV2 with ATF3-specific siRNAs (S1, S2 and S3) and negative control siRNA, and harvested at DIV3. Western blot analysis was performed. (A) Membranes were immunolabeled with ATF3-specific antibody. Numbers on the left indicate the protein mass of the ladder bands in kDa. (B) 14 kDa ATF3 isoform expression. (C) 22 kDa ATF3 isoform expression. (D) 25 kDa ATF3 form expression. GAPDH was a loading control.*

In P16-18 cultures (Figure 25), the expression of 14 kDa ATF3 isoform was increased in all treated samples: ATF3 S1 +44.90%, ATF3 S2 +30.40%, ATF3 S3 +31.80% and negative control +14.40% (Figure 25B). The other isoform, 22 kDa in size, was expressed more in samples treated with ATF3 S1 and S3 siRNAs, by 14.20% and 39.60%, respectively, and remained almost the same in ATF3 S2 siRNA-treated samples, -2.90%. In negative control samples the expression was 44.53% lower than in untreated samples (Figure 25C). Similarly, the expression of 25 kDa ATF3 form (Figure 25D) was increased in ATF3 S1 (+22.30%) and S3 (+12.20%) siRNA-treated samples, and it remained almost the same in ATF3 S2 siRNA-treated samples, -3.70%. Again, the expression in negative control samples (-28.20%) was lower than in the control. The 30 kDa ATF3 form expression was increased in all siRNA-treated samples: ATF3 S1 +86.70%, ATF3 S2 +36.10%, ATF3 S3 +36.60% and negative control +26.20%

(Figure 25E). Finally, the expression of the 35 kDa ATF3 form (Figure 25F) was increased in ATF3 S1-3 siRNA-treated samples, +49.40%, +10.80% and 46.10%, respectively. In the negative control samples, the expression was unchanged (-0.20%).

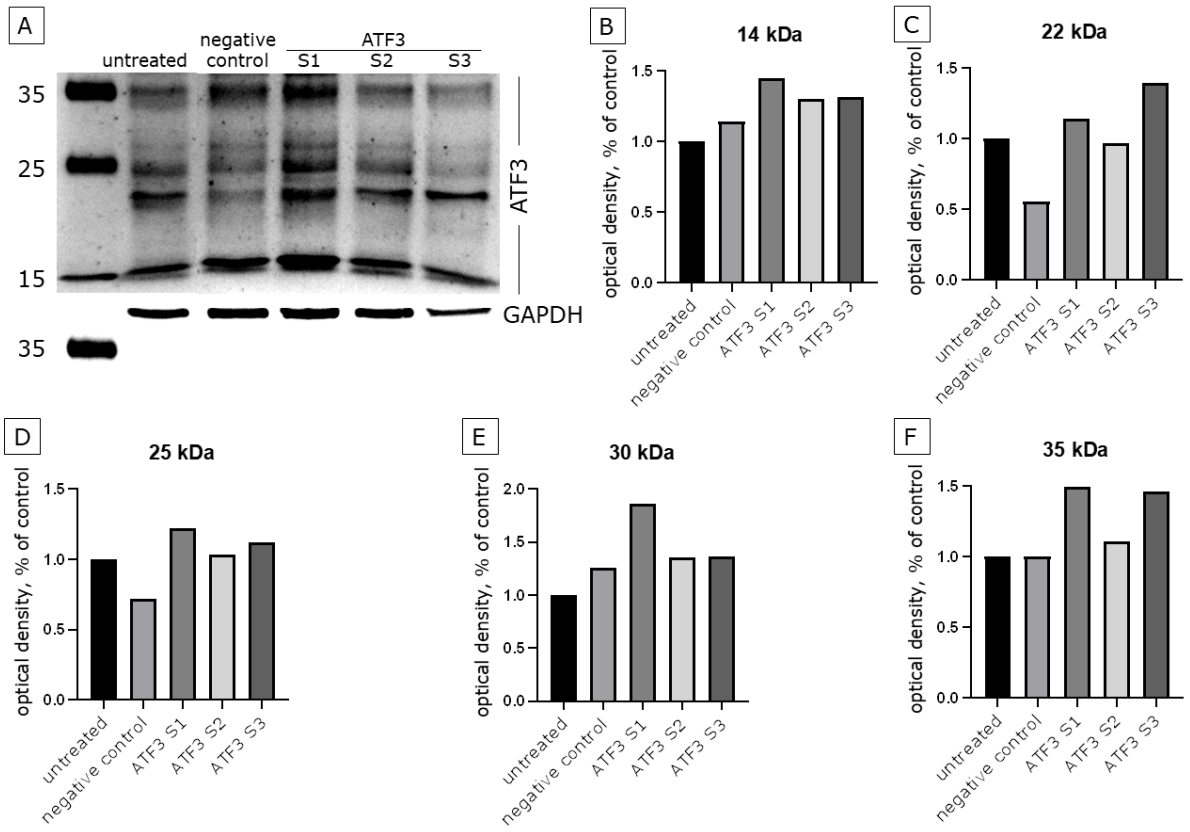

Figure 25 ***Expression levels of ATF3 (iso)forms in P16-18 cultures after ATF3 silencing.*** *P16-18 cultures were treated at DIV1 and DIV2 with ATF3-specific siRNAs (S1, S2 and S3) and negative control siRNA. Cells were harvested at DIV3 and Western blot analysis was performed. (A) Membranes were immunolabeled with ATF3-specific antibody. Numbers on the left indicate the protein mass of the ladder bands in kDa. (B) 14 kDa ATF3 isoform expression. (C) 22 kDa ATF3 isoform expression. (D) 25 kDa ATF3 form expression. (E) 30 kDa ATF3 form expression. (F) 35 kDa ATF3 form expression. GAPDH was a loading control.*

5. DISCUSSION

Regeneration of the CNS is investigated in animal models that have the highest genetic homology with humans to obtain the highly translatable results. However, adult mammals are often inefficient in compensating for the extensive loss of neurons resulting from various experimental procedures (16). Since mammals are both difficult and costly to maintain as laboratory animals, much research on CNS regeneration has been conducted on non-mammals, such as amphibians (37), or teleost fish (38). Amphibians are useful for research and better understanding of molecular pathways and factors, although, despite remarkable regenerative capacities, they lack genetic homology with humans. Therefore, all findings from experiments on the lower vertebra must be confirmed in mammals before translation into clinical settings (16).

The most widely used platform for *in vitro* research are cell cultures. In general, they are easier to manipulate and maintain than living animals. Experimental conditions can be better controlled, and thus, cell cultures offer greater reproducibility (39). There are three main types of cell cultures used: immortalized cell lines, primary cell cultures and induced pluripotent stem cells (iPSCs). The most common cell lines used in neuroregeneration research are SH-SHY5Y (40), NT2 (41), PC12 (42) and NSC-34 (43). Their advantages are renewability, homogeneity (they represent one type of cell), and easier long-term culturing and maintenance. Nevertheless, they do not recapitulate the properties of *in vivo* neurons well. Primary neuronal cells, on the other hand, retain most of the characteristics and genetic information as *in vivo* neurons, which makes data obtained from them more reliable. However, primary cultures are generally harder to prepare than cell lines and yield a limited number of cells. Working with primary neuronal cell cultures is even more challenging since neurons are post-mitotic cells. Lately, reprogramming patients' somatic cells into iPSCs is used to generate patient-specific iPSCs that could be differentiated into cell types relevant to

the investigated disease. Paşca et al. (44) derived iPSCs from the patient who suffered from Timothy syndrome and differentiated them into neurons. This relatively new approach enables investigation of exact pathological changes and/or mutations present in the patient's cells.

In this work, given the need for a new, more affordable, and simpler mammalian model for investigating neuronal regeneration, long-term primary cortical cell cultures from neonatal opossums, *Monodelphis domestica*, were successfully prepared.

There are numerous advantages for using *M. domestica* as a source of primary neurons and other CNS cells. Firstly, *M. domestica* are marsupials without a pouch (17) that give birth to very immature pups. Opossum neonates' CNS has embryonic-like characteristics (17) and CNS development can be investigated in postnatal opossums. Furthermore, they are easy to maintain as laboratory animals, since they breed relatively often and during the whole year (18). Finally, opossums regenerate spinal cord after injury in the first two weeks of their life (21,22).

However, working with opossums has brought some challenges. For immunofluorescence assays, most antibodies available on the market are designed to work in rodents, like mice and rats, or in humans. For every antibody that was used in this research, alignment of opossum protein with the immunogen was performed, if data were available. Fortunately, opossums have high protein sequence homology with other mammalian species, including rodents and humans. Furthermore, commercially available positive control siRNA used in silencing protocol optimization is specific to the human ACTB gene transcript. Positive controls were available from different manufacturers against human, mouse and rat, but none were found against opossum gene transcripts.

The primary cortical cultures derived from P3-5 opossums characterized in this work are almost completely neuronal for up to 3 weeks *in vitro*. After 4 days *in vitro*, nearly 98% of the cells express at least one

neuronal marker, TUJ1, MAP2 or NeuN, with more than 93% of cells being positive for all three. More than 80% of all cells in the culture are neurons until DIV22, when they decrease to nearly 65%. Opossums that are 3-5 days old developmentally correspond to E15.5-18.5 rat or E14-16 mouse embryos (20), from which cortical cultures with similar characteristics are obtained. For instance, Xu et al. (45) prepared primary cortical culture with more than 95% neuronal cells from embryonic E18 rat.

In P3-5 cultures, growth cones were detected. GCs are structures rich in actin that are involved in axon guidance and result in formation of the axon. The presence of axon in DIV4, but not in DIV1, indicates that neurons thrive to form connections in culture. Immunostaining of P3-5 cells with anti-synapsin I at DIV15 confirmed formation of synapses *in vitro*. In Petrović et al. (31), it was additionally shown that cultured primary neurons express excitatory and inhibitory synaptic markers such as vGLUT2 and GAD65, respectively. The expression of these synaptic markers has also been previously demonstrated in the opossum spinal cord (34). Together with the establishment of neuronal networks, these results indicate that primary opossum cortical culture resembles tissue well in the context of cell development and composition.

Primary cortical cultures were also prepared from P16-18 opossums, which do not regenerate their spinal cord after injury. Compared to P3-5, P16-18 cultures had a lower proportion of neurons throughout the period observed. At DIV15, the percentage of neurons decreased to roughly 55%. Non-neuronal cells were more abundant than in P3-5 cultures, which was expected due to ongoing CNS maturation in opossums and the appearance of glial cells (18).

In both age groups, cells migrate and form 3D neuronal clusters during the second week *in vitro*. CNS cells naturally do not grow in a monolayer like they do when cultured. In tissue, they spread processes in all three dimensions and form connections, and thus, in culture they tend

to form aggregates. A similar observation was described by Todd et al. (46) in primary mouse hippocampal neuronal culture.

RGCs are the main progenitor population of all CNS cell lineages, and their role in the development of cortical tissue has been described (14,15). In P3-5 cultures, RGCs proliferate *in vitro* when maintained in proliferative medium. Petrović et al. (31) presented that opossum RGCs could be passaged multiple times for more than a month, and that in different medium, they differentiate *in vitro* into neurons or glial cells.

In the second part of this work, the goal was to genetically silence ATF3, a molecule important in neuroregeneration, and to confirm it at the level of mRNA and protein. The method of choice was transfection of cells with ATF3-specific siRNAs. There is only one report of transfection of primary opossum cortical cultures by Bartkowska et al. (47), but in this case, the cells were transfected with plasmids carrying shRNA.

In P3-5 cultures, silencing of ATF3 was partially successful. Silencing was confirmed on the mRNA level, but the results were not as expected. Levels of ATF3 gene transcript 201 were equally reduced in all samples, by about 50%. However, when expression of both gene transcripts was tested simultaneously, S3 siRNA should have shown stronger effect than the other siRNAs, because it is designed to target both transcripts, while S1 and S2 siRNAs target only the 201 gene transcript. The experiment was conducted once in P3-5 cultures, and it must be repeated before making conclusions.

Western blot results showed that, all ATF3-specific siRNAs (S1, S2, S3) caused 34-50% reduction in the expression of the 14 kDa ATF3 isoform, but it was expected that only ATF3 S3 siRNA would have an effect. Next, all siRNAs should have targeted 22 kDa ATF3 isoform expression. In contrast, the expression of this isoform was unchanged after transfection with S1 and S2 siRNAs, and only the S3 siRNA caused the decrease in protein expression. Moreover, there was an additional form of ATF3 detected in P3-5 cultures, at approximately 25 kDa in size, and its

expression increased when transfected with siRNAs. A possible explanation for observed changes is that 25 kDa ATF3 isoform has a posttranslational modification (see Introduction), and that transfection does not decrease the net amount of protein available in the cell. Instead, with decreased ATF3 mRNA levels, post translationally modified form may be favored over the native protein form.

In P16-18 cultures, silencing of ATF3 was not successful at the mRNA level. Levels of the ATF3 201 transcript was slightly reduced in all ATF3 and negative control siRNA-treated samples. However, the decrease was less than 11%, so the expression can be considered to have remained unchanged. ATF3 202 transcript was decreased for less than 17% in every ATF3 siRNA-treated sample. Like in P3-5 cultures, there was no difference in sample treated with ATF3 S3 siRNA. In negative control sample, the expression increased by 15%.

During the optimization of the ATF3 silencing protocol, the existence of additional isoforms in P16-18 samples was detected. From then on, we focused on all of these ATF3 isoforms.

Expression of all detected protein forms in P16-18 samples was increased from 14% to nearly 90% in ATF3 S1 siRNA-treated samples. In samples treated with ATF3 S2 siRNA, 22 and 25 kDa ATF3 (iso)forms remained unchanged, while the expression of other detected forms increased to 10-36%. In all samples treated with ATF3 S3 siRNA, all ATF3 protein forms were expressed more (12-46%) than in the control sample, while it was expected that 14 and 22 kDa isoform expressions will be reduced.

These unexpected outcomes could be due to several probable reasons. Firstly, this is the first attempt of gene silencing in primary opossum cortical cultures using siRNA, and further optimization might be needed. Secondly, silencing of the ATF3 gene should be repeated in cell cultures of both ages to get statistically significant results. Finally, there

are some indications in these preliminary results that transfection is more effective in cultures derived from younger P3-5 opossums. Thus, cells of the P16-18 cultures could be too differentiated to be transfected successfully. Alabdullah et al. (48) reported that transfection can be up to 10 times less efficient in differentiated, as opposed to undifferentiated, neural cells.

Until now, ATF3-specific siRNAs were used only individually. Neumeier and Meister (49) have recently published a mini review of RNAi mechanisms and strategies that are used to reduce off-target effects. They emphasized that a relatively high siRNA concentration is used when they are used individually, which increases the possibility of off-target effects. Pooling siRNAs might be a solution to make transfections more targeted. Thus, in further research, we will try to transfect cells with combinations of two or three siRNAs and evaluate whether some of the combinations show additive or synergistic effects.

Upon successful method optimization and confirmation of silencing, neuroregeneration scratch assay will be performed in cell cultures of both ages. We already introduced and described this assay in Petrović et al., unpublished data. Briefly, cells are plated on 12 mm diameter glass coverslips and maintained in culture as described in Materials and Methods. When neuronal networks are established, a scratch 0.1 mm wide is made through the middle of the coverslip using fine-tip tweezers. The scratch injures differentiated neurons. Neurite outgrowth and/or neuronal regeneration are observed, measured, and quantified after 24 and 48 h.

The current plan is to silence the ATF3 gene when the neuronal networks are well established, approximately at DIV10, and to perform a scratch assay on the next day to test regenerative abilities of neurons in treated vs. untreated samples.

6. CONCLUSIONS

In this work, characterization of primary cortical cell cultures from *Monodelphis domestica* is presented. The whole process, and information obtained, were recently published in Frontiers in Cellular Neuroscience (31), but this work contains additional analyses and procedures that are not described elsewhere.

We have demonstrated that by using different experimental procedures and media enrichment of different CNS cell types can be obtained in the culture. Briefly, an almost pure neuronal culture was obtained with use of neuronal medium, while the proportion of proliferative cells, such as radial glial cells, was increased using a proliferative medium. In further procedures, we are eager to establish cultures of primary cortical astrocytes, and primary cell cultures from the opossum spinal cord.

We showed axonal growth and establishment of neuronal networks in cultures from two developmentally different ages, P3-5 and P16-18. Moreover, it was proven that synapses and growth cones formation also occur *in vitro*.

In opossum P3-5 and P16-18 cultures, the optimization of gene silencing using ACTB- and ATF3-specific siRNAs was performed. This is the first report of siRNA transfection of primary opossum cortical cell cultures. Transfection of the cells with fluorescently labeled siRNA, that enables visualization of transfected cells, confirmed that siRNA enters the cells. In the first experiment, silencing of ATF3 in P3-5 cultures was partially successful at the mRNA and protein level.

Results of this work suggest that opossum-derived primary cortical cultures can be used to investigate mechanisms of CNS regeneration and the role of regeneration-related transcription factors such as ATF3.

7. REFERENCES

1. Bear MF, Connors BW, Paradiso MA. Neuroscience: exploring the brain. 4th ed. Wolters Kluwer. 2016.
2. Stoker TB, Torsney KM, Barker RA. Emerging treatment approaches for Parkinson's disease. Front Neurosci. 2018;12(OCT):1–10.
3. Alexopoulos GS. Mechanisms and treatment of late-life depression. Transl Psychiatry [Internet]. 2019;9(1). Available from: http://dx.doi.org/10.1038/s41398-019-0514-6
4. Yang AC, Tsai SJ. New targets for schizophrenia treatment beyond the dopamine hypothesis. Int J Mol Sci. 2017;18(8).
5. Cummings JL, Tong G, Ballard C. Treatment Combinations for Alzheimer's Disease: Current and Future Pharmacotherapy Options. J Alzheimer's Dis. 2019;67(3):779–94.
6. Fernández-Susavila H, Bugallo-Casal A, Castillo J, Campos F. Adult stem cells and induced pluripotent stem cells for stroke treatment. Front Neurol. 2019;10(AUG).
7. Louveau A, Harris TH, Kipnis J. Revisiting the Mechanisms of CNS Immune Privilege. Trends Immunol [Internet]. 2015;36(10):569–77. Available from: http://dx.doi.org/10.1016/j.it.2015.08.006
8. Erkkinen MG, Kim M, Geschwind MD. Clinical Neurology and Epidemiology of the Major Neurodegenerative Diseases. Cold Spring Harb Lab Press. 2018;
9. Bajwa NM, Kesavan C, Mohan S. Long-term consequences of Traumatic brain injury in bone metabolism. Front Neurol. 2018;9(MAR):1–9.
10. Alizadeh A, Dyck SM, Karimi-Abdolrezaee S. Traumatic spinal cord injury: An overview of pathophysiology, models and acute injury

mechanisms. Front Neurol. 2019;10(March):1–25.

11. James SL, Bannick MS, Montjoy-Venning WC, Lucchesi LR, Dandona L, Dandona R, et al. Global, regional, and national burden of traumatic brain injury and spinal cord injury, 1990-2016: A systematic analysis for the Global Burden of Disease Study 2016. Lancet Neurol. 2019;18(1):56–87.

12. Kaur P, Sharma S. Recent Advances in Pathophysiology of Traumatic Brain Injury. Curr Neuropharmacol. 2017;16(8):1224–38.

13. Wheaton BJ, Sena J, Sundararajan A, Umale P, Schilkey F, Miller RD. Identification of regenerative processes in neonatal spinal cord injury in the opossum (Monodelphis domestica): A transcriptomic study. J Comp Neurol. 2020;

14. Götz M, Barde YA. Radial glial cells: Defined and major intermediates between embryonicstem cells and CNS neurons. Neuron. 2005;46(3):369–72.

15. Götz M, Stoykova A, Gruss P. Pax6 controls radial glia differentiation in the cerebral cortex. Neuron. 1998;21(5):1031–44.

16. Vijayanathan Y, Lim SM, Tan MP, Lim FT, Majeed ABA, Ramasamy K. Adult Endogenous Dopaminergic Neuroregeneration Against Parkinson's Disease: Ideal Animal Models? Neurotox Res [Internet]. 2021;39(2):504–32. Available from: https://doi.org/10.1007/s12640-020-00298-7

17. Macrini TE. Monodelphis domestica. Mamm Species. 2004;760(760):1–8.

18. Saunders NR, Adam E, Reader M, Møllgård K. Monodelphis domestica (grey short-tailed opossum): an accessible model for studies of early neocortical development. Anat Embryol (Berl). 1989;180(3):227–36.

19. Puzzolo E, Mallamaci A. Cortico-cerebral histogenesis in the opossum

Monodelphis domestica: Generation of a hexalaminar neocortex in the absence of a basal proliferative compartment. Neural Dev. 2010;5(1):1–18.

20. Cardoso-Moreira M, Halbert J, Valloton D, Velten B, Chen C, Shao Y, et al. Gene expression across mammalian organ development. Nature. 2019;571(7766):505–9.

21. Saunders NR, Deal A, Knott GW, Varga ZM, Nicholls JG. Repair and Recovery Following Spinal Cord Injury in a Neonatal Marsupial (Monodelphis Domestica). Clin Exp Pharmacol Physiol. 1995;22(8):518–26.

22. Fry EJ, Stolp HB, Lane MA, Dziegielewska KM, Saunders NR. Regeneration of Supraspinal Axons after Complete Transection of the Thoracic Spinal Cord in Neonatal Opossums (Monodelphis domestica). J Comp Neurol. 2003;466(3):422–44.

23. Chen BPC, Liang G, Whelan J, Hai T. ATF3 and ATF3ΔZip. Transcriptional repression versus activation by alternatively spliced isoforms. J Biol Chem. 1994;269(22):15819–26.

24. Howe KL, Achuthan P, Allen J, Allen J, Alvarez-Jarreta J, Ridwan Amode M, et al. Ensembl 2021. Nucleic Acids Res. 2021;49(D1):D884–91.

25. Seijffers R, Zhang J, Matthews JC, Chen A, Tamrazian E, Babaniyi O, et al. ATF3 expression improves motor function in the ALS mouse model by promoting motor neuron survival and retaining muscle innervation. Proc Natl Acad Sci U S A. 2014;111(4):1622–7.

26. Campbell G, Hutchins K, Winterbottom J, Grenningloh G, Lieberman AR, Anderson PN. Upregulation of activating transcription factor 3 (ATF3) by intrinsic CNS neurons regenerating axons into peripheral nerve grafts. Exp Neurol. 2005;192(2):340–7.

27. Zhang SJ, Buchthal B, Lau D, Hayer S, Dick O, Schwaninger M, et al.

A signaling cascade of nuclear calcium-CREB-ATF3 activated by synaptic NMDA receptors defines a gene repression module that protects against extrasynaptic NMDA receptor-induced neuronal cell death and ischemic brain damage. J Neurosci. 2011;31(13):4978–90.

28. Kramer NJ, Haney MS, Morgens DW, Jovičić A, Couthouis J, Li A, et al. CRISPR-Cas9 screens in human cells and primary neurons identify modifiers of C9ORF72 dipeptide-repeat-protein toxicity. Nat Genet. 2018;50(4):603–12.

29. Blanquie O, Bradke F. Cytoskeleton dynamics in axon regeneration. Curr Opin Neurobiol [Internet]. 2018;51:60–9. Available from: https://doi.org/10.1016/j.conb.2018.02.024

30. Chong ZX, Yeap SK, Ho WY. Transfection types, methods and strategies: A technical review. PeerJ. 2021;9:1–37.

31. Petrović A, Ban J, Tomljanović I, Pongrac M, Ivaničić M, Mikašinović S, et al. Establishment of Long-Term Primary Cortical Neuronal Cultures From Neonatal Opossum Monodelphis domestica. Front Cell Neurosci. 2021;15(March):1–15.

32. Mladinic M, Bianchetti E, Dekanic A, Mazzone GL, Nistri A. ATF3 is a novel nuclear marker for migrating ependymal stem cells in the rat spinal cord. Stem Cell Res [Internet]. 2014;12(3):815–27. Available from: http://dx.doi.org/10.1016/j.scr.2014.03.006

33. Untergasser A, Cutcutache I, Koressaar T, Ye J, Faircloth BC, Remm M, et al. Primer3-new capabilities and interfaces. Nucleic Acids Res. 2012;40(15):1–12.

34. Petrovic A, Veeraraghavan P, Olivieri D, Nistri A, Jurcic N, Mladinic M. Loss of inhibitory synapses causes locomotor network dysfunction of the rat spinal cord during prolonged maintenance in vitro. Brain Res [Internet]. 2019;1710:8–21. Available from: https://doi.org/10.1016/j.brainres.2018.12.029

35. Cullen DK, Gilroy ME, Irons HR, Laplaca MC. Synapse-to-neuron ratio is inversely related to neuronal density in mature neuronal cultures. Brain Res [Internet]. 2010;1359:44–55. Available from: http://dx.doi.org/10.1016/j.brainres.2010.08.058

36. Madeira F, Park YM, Lee J, Buso N, Gur T, Madhusoodanan N, et al. The EMBL-EBI search and sequence analysis tools APIs in 2019. Nucleic Acids Res. 2019;47(W1):W636–41.

37. O'Hara CM, Egar MW, Chernoff EAG. Reorganization of the ependyma during axolotl spinal cord regeneration: Changes in intermediate filament and fibronectin expression. Dev Dyn. 1992;193(2):103–15.

38. Bhattarai P, Thomas AK, Zhang Y, Kizil C. The effects of aging on Amyloid-β42-induced neurodegeneration and regeneration in adult zebrafish brain. Neurogenesis [Internet]. 2017;4(1):e1322666. Available from: https://doi.org/10.1080/23262133.2017.1322666

39. Lindhorst PH, Hummon AB. Proteomics of Colorectal Cancer: Tumors, Organoids, and Cell Cultures—A Minireview. Front Mol Biosci. 2020;7(December).

40. Xicoy H, Wieringa B, Martens GJM. The SH-SY5Y cell line in Parkinson's disease research: a systematic review. Mol Neurodegener [Internet]. 2017;12(1):1–11. Available from: http://dx.doi.org/10.1186/s13024-017-0149-0

41. Roloff F, Scheiblich H, Dewitz C, Dempewolf S, Stern M, Bicker G. Enhanced neurite outgrowth of human model (NT2) neurons by small-molecule inhibitors of Rho/ROCK signaling. PLoS One. 2015;10(2):1–14.

42. Zheng Z, Huang L, Yan L, Yuan F, Wang L, Wang K, et al. Polyaniline functionalized graphene nanoelectrodes for the regeneration of PC12 cells via electrical stimulation. Int J Mol Sci. 2019;20(8).

43. Nango H, Kosuge Y, Yoshimura N, Miyagishi H, Kanazawa T, Hashizaki

K, et al. The Molecular Mechanisms Underlying Prostaglandin D2-Induced Neuritogenesis in Motor Neuron-Like NSC-34 Cells. Cells. 2020;9(4):1–16.

44. Pasca SP, Portmann T, Voineagu I, Yazava M, Shcheglovitov O et al. Using iPSC-derived neurons to uncover cellular phenotypes associated with Timothy Syndrome. Nat Med. 2011;17(3):1657–63.

45. Xu SY, Wu YM, Ji Z, Gao XY, Pan SY. A modified technique for culturing primary fetal rat cortical neurons. J Biomed Biotechnol. 2012;2012(c).

46. Todd GK, Boosalis CA, Burzycki AA, Steinman MQ, Hester LD, Shuster PW, et al. Towards Neuronal Organoids: A Method for Long-Term Culturing of High-Density Hippocampal Neurons. PLoS One. 2013;8(4):1–13.

47. Bartkowska K, Gajerska M, Turlejski K, Djavadian RL. Expression of TrkC Receptors in the Developing Brain of the Monodelphis opossum and Its Effect on the Development of Cortical Cells. PLoS One. 2013;8(9):1–14.

48. Alabdullah AA, Al-Abdulaziz B, Alsalem H, Magrashi A, Pulicat SM, Almzroua AA, et al. Estimating transfection efficiency in differentiated and undifferentiated neural cells. BMC Res Notes [Internet]. 2019;12(1):1–7. Available from: https://doi.org/10.1186/s13104-019-4249-5

49. Neumeier J, Meister G. siRNA Specificity: RNAi Mechanisms and Strategies to Reduce Off-Target Effects. Front Plant Sci. 2021;11(January):1–7.

FUNDING

Experimental part of this work was conducted on equipment financed by the European Regional Development Fund (ERDF) within the project "Research Infrastructure for Campus-based Laboratories at University of Rijeka" (RC.2.2.06-0001), the Croatian Science Foundation (CSF) grant IP-2016-06-7060, the financial support from the University of Rijeka (Ban, J: uniri-prirod-18-290; Mladinic, M: uniri-biomed-18-258), and from the International Centre for Genetic Engineering and Biotechnology (ICGEB), Grant/Award Number: CRP/CRO14-03.